Cerebral Cortex October 2010;20:2333–2347
doi:10.1093/cercor/bhp310
Advance Access publication January 18, 2010

Serotonin 3A Receptor Subtype as an Early and Protracted Marker of Cortical Interneuron Subpopulations

Ksenija Vucurovic[1,2], Thierry Gallopin[1], Isabelle Ferezou[1], Armelle Rancillac[1], Pascal Chameau[3], Johannes A. van Hooft[3], Hélène Geoffroy[1], Hannah Monyer[4], Jean Rossier[1] and Tania Vitalis[1,2]

[1]CNRS-UMR 7637, Laboratoire de Neurobiologie, ESPCI ParisTech, 75005 Paris, France, [2]INSERM U616, Développement Normal et Pathologique du Cerveau, Hôpital de la Salpétrière, 75013 Paris, France, [3]University of Amsterdam, Swammerdam Institute for Life Sciences, Section Neurobiology, Center for Neuroscience, NL-1090 GB Amsterdam, The Netherlands and [4]Department of Clinical Neurobiology, Interdisziplinaeres Zentrum fuer Neurowissenschaften, University of Heidelberg, Heidelberg, Germany

Ksenija Vucurovic, Thierry Gallopin, and Isabelle Ferezou contributed equally.

Address correspondence to Tania Vitalis, CNRS-UMR 7637, Laboratoire de Neurobiologie, ESPCI ParisTech, 10 rue Vauquelin, 75005 Paris, France. Email: tania.vitalis@espci.fr.

To identify neocortical neurons expressing the type 3 serotonergic receptor, here we used transgenic mice expressing the enhanced green fluorescent protein (GFP) under the control of the 5-HT_{3A} promoter (5-HT_{3A}:GFP mice). By means of whole-cell patch-clamp recordings, biocytin labeling, and single-cell reversed-transcriptase polymerase chain reaction on acute brain slices of 5-HT_{3A}:GFP mice, we identified 2 populations of 5-HT_{3A}-expressing interneurons within the somatosensory cortex. The first population was characterized by the frequent expression of the vasoactive intestinal peptide and a typical bipolar/bitufted morphology, whereas the second population expressed predominantly the neuropeptide Y and exhibited more complex dendritic arborizations. Most interneurons of this second group appeared very similar to neurogliaform cells according to their electrophysiological, molecular, and morphological properties. The combination of 5-bromo-2-deoxyuridine injections with 5-HT_{3A} mRNA detection showed that cortical 5-HT_{3A} interneurons are generated around embryonic day 14.5. Although at this stage the 5-HT_{3A} receptor subunit is expressed in both the caudal ganglionic eminence and the entopeduncular area, homochronic in utero grafts experiments revealed that cortical 5-HT_{3A} interneurons are mainly generated in the caudal ganglionic eminence. This protracted expression of the 5-HT_{3A} subunit allowed us to study specific cortical interneuron populations from their birth to their final functional phenotype.

Keywords: development, GABA, 5-HT_{3A}, NPY, VIP

Introduction

The cerebral cortex is the main integrative center of higher-order cognitive functions. It processes information through a complex neuronal network comprising efferent excitatory pyramidal cells and GABAergic inhibitory interneurons. Although they represent a minority of cells in the cortex, interneurons are key coordinators of intercellular communications and serve a crucial role in modulating neuronal output via the release of γ-aminobutyric acid (GABA) and neuropeptides (Baraban and Tallent 2004). The intrinsic properties of these neurons are highly diverse, suggesting the existence of distinct classes of interneurons exerting specific functions within the cortical network. Indeed, cortical interneurons are typically described and classified according to their morphological, physiological, and molecular characteristics, and to their connectivity (DeFelipe 1993; Cauli et al. 1997; Gupta et al. 2000; Kawaguchi and Kondo 2002; Ascoli et al. 2008). Interestingly, the diversity of cortical interneurons appears to rely on differential developmental ontogeny that is becoming another obvious criterion of their classification and could help to understand their functional specificity.

In rodents, unlike in humans or primates (Letinic et al. 2002), telencephalic interneurons mainly derive from the anlagen of the basal telencephalon (Corbin et al. 2001; Marín and Rubenstein 2001). In vitro studies of cortical interneurons migration (Lavdas et al. 1999; Wichterle et al. 1999) and fate-mapping experiments (Xu et al. 2003) have shown that the ganglionic eminences (lateral [LGE], medial [MGE], and caudal [CGE]) are the principal sources of cortical interneurons (Nery et al. 2002; Xu et al. 2003). Previous reports have also indicated the contribution of several other regions such as the entopeduncular area (AEP, Anderson et al. 2001) and the preoptic area (Gelman et al. 2009), albeit little is known about their potential to generate distinct telencephalic interneurons. Compelling evidence is suggesting that the commitment of 1 interneuron subtype is linked to its birth date and location within a particular region of the basal telencephalon. Indeed, in vivo fate-mapping experiments suggest that cortical parvalbumin (Parv)- and somatostatin (SOM)-expressing subtypes of interneurons arise mainly from the MGE/AEP, whereas a large proportion of interneurons containing vasoactive intestinal peptide (VIP) and/or calretinin (CR) are predominantly generated in the CGE (Nery et al. 2002; Butt et al. 2005).

In the telencephalon, like in the spinal cord, unique combinations of transcription factors expressed by progenitor cells specify the identity of each class of interneurons that derive from individual progenitor domains (Jessell 2000; Schuurmans and Guillemot 2002). Most transcription factors are turned off in part or entirely at postnatal stages (such as Lhx6 or Nkx2.1) when interneurons are mature and express neurochemical markers generally used for their classification (Cobos et al. 2006). So far, only few molecular markers have been identified as continuously expressed by a distinct subtype of interneurons from the embryonic period to adulthood. By using bacterial artificial chromosome (BAC) transgenic mice expressing enhanced green fluorescent protein (GFP) under the control of the 5-HT_{3A} promoter (5-HT_{3A}) and homochronic in utero grafts of 5-HT_{3A}:GFP+ cells, we provide evidence that the 5-HT_{3A} receptor is protractedly expressed from early postmitotic stages by 2 subtypes of cortical interneurons exhibiting distinctive morphological, molecular, and physiological properties.

Materials and Methods

Animals

Animal procedures were conducted in strict compliance with approved institutional protocols and in accordance with the provisions for animal care and use described in the European Communities Council directive of 24 November 1986 (86-16-09/EEC). The day of vaginal plug detection was counted as embryonic day (E) E 0.5. Two transgenic mouse lines expressing the enhanced GFP under the control of the 5-HT_{3A} (5-HT_{3A}:GFP) obtained by using modified BACs were used: The first one has been generated in H. Monyer's laboratory (Inta et al. 2008), was maintained under the C57/Bl6 background, and was mainly used to assess the feasibility of the project. The second transgenic mouse line Tg(Htr3a-GFP)1Gsat was provided by the GENSAT Consortium (Rockeffeler University-GENSAT Consortium; Heintz 2004) and was maintained under the Swiss background. Both strains gave identical expression patterns in cortical areas and match mRNAs expression. Genitors were polymerase chain reaction (PCR) genotyped for GFP insertion using the primers (from 5′ to 3′): ATGGTGAGCAAGGGC-GAGGAGCT and GCCGAGAGTGATCCCGGCGGCGGT. Embryos were phenotyped by macroscopic observation under fluorescent optics. Characterization of juvenile 5-HT_{3A}-expressing interneurons was performed using the Tg(Htr3a-GFP) mouse line provided by GENSAT. Both the GENSAT and Hannah Monyer's mouse lines were used for analysis of embryonic GFP expression and grafting experiments and gave similar results.

Radioactive In Situ Hybridization

5-HT_{3A} cRNA probe corresponded to the full-length domain of the protein. The plasmid was linearized with *Bam*H1 for antisense RNA synthesis by T7 polymerase and with *Eco*RI for sense RNA synthesis by T3 polymerase. The *Dlx2* cRNA probe (*Hin*d3 linearization, T7 polymerization) was also used. The transcription was carried out using the Promega kit, and probes were labeled with ^{35}S-UTP (>1000 Ci/mmol; Amersham). Hybridization was performed on fresh frozen brain sections (15 μm thick) as previously described (Fontaine and Changeux 1989). Slides were dipped in photographic emulsion (NTB2, Kodak) and exposed for about 5–10 days. Emulsions were then developed, and sections were Nissl counterstained (0.25 % thionin solution).

The laminar density of cells expressing the 5-HT_{3A} mRNA was estimated at P25. Quantifications of 5-HT_{3A}+ cells were performed at the level of the primary somatosensory cortex, in 500-μm-wide cortical strips (data are expressed as percentage). Three adjacent sections of at least 5 independent preparations were used.

Immunohistochemistry

Neuronal populations expressing 5-HT_{3A}:GFP were analyzed at embryonic (E13/E13.5 [n = 8], E14.5 [n = 12], E15.5 [n = 8], E16.5 [n = 12], E17.5 [n = 10], and E18.5 [n = 10]), and postnatal stages (P0 [n = 14], P1 [n = 8], P3 [n = 10], P5 [n = 6], P15–P16 [n = 10], and P25 [n = 14]). Embryos collected by cesarean section after cervical dislocation of the dam were placed overnight in 4% paraformaldehyde in 0.1 M phosphate buffer (PB), pH 7.4 (PFA). Embryos were cryoprotected, embedded into gelatine (7%)–sucrose (10%), frozen into isopentane (−40°C) and sectioned coronally (20 μm) with a cryostat. Postnatal animals were deeply anesthetized with an intraperitoneal (IP) injection of pentobarbital (150 mg/kg body weight) and perfused transcardially with 4% PFA. Postnatal brains were cryoprotected in 30% sucrose and cut on a freezing microtome (35 μm). For immunofluorescence, sections were incubated overnight at 4 °C with the following antibodies diluted in saline PB (PBS): rabbit anti-CR (1:8000, Swant), rabbit anti-Parv (1:1000; Swant), rabbit anti-SOM (1:500; a kind gift of Dr Epelbaum), rabbit anti-NPY (neuropeptide Y) (1:500, Amersham), rabbit anti-VIP (1:800, Incstar), rabbit anti-Nr2F2 (1:200; Acris GmbH), rabbit anti-GABA (1:5000; Sigma), rabbit anti-GFP (1:1000, Molecular Probes), mouse anti-tuj1 (1:2000, Babco), or mouse anti-Parv (1:200, Sigma). After washing in PBS, sections were incubated with Cy3-conjugated goat antirabbit or/and antimouse antibodies (1:200; Jackson Laboratory). Sections were rinsed in PB, mounted in Vectashield (Vector) containing 4′,6′-diamidino-2-phénylindole (Dapi) and were observed with a fluorescent microscope (Leica, DMR). Images were acquired with a Coolsnap camera (Photometrics, Tucson, AZ) and analyzed with the Metamorph software (Molecular Devices, Foster City, CA).

The laminar density of cells expressing GFP was estimated at P25. Quantifications of GFP:5-HT_{3A}+ cells were performed at the level of the primary somatosensory cortex, in 500-μm-wide cortical strips (data are expressed as percentage). Three adjacent sections of at least 5 independent preparations were used.

The proportion of green fluorescent cells labeled for GABA at E14.5 (n = 9) in the low intermediate zone (LIZ) was estimated at 2 different levels, 1 rostral including MGE and 1 caudal including CGE. For each case, data obtained from 3 adjacent sections were averaged.

Preparation of Juvenile Brain Slices and Electrophysiological Recordings of 5-HT_{3A}-Expressing Cells

5-HT_{3A}:GFP transgenic mice (postnatal days 14–18) were decapitated, brains were quickly removed and placed into cold (~4 °C) artificial cerebrospinal fluid (ACSF) containing (in mM): 110 choline chloride, 11.6 Na-ascorbate, 7 $MgCl_2$, 2.5 KCl, 1.25 NaH_2PO_4, and 0.5 $CaCl_2$, continuously bubbled with 95%O_2–5%CO_2. Coronal brain slices (300 μm thick) containing the somatosensory cortex were cut with a vibratome (VT1200S; Leica, Nussloch, Germany), and transferred to a holding chamber containing ACSF (in mM): 126 NaCl, 2.5 KCl, 1.25 NaH_2PO_4, 2 $CaCl_2$, 1 $MgCl_2$, 26 $NaHCO_3$, 20 glucose, and 1 kynurenic acid (nonspecific glutamate receptor antagonist, Sigma), constantly oxygenated (95% O_2/5% CO_2) and held at room temperature.

Individual slices were placed in a submerged recording chamber and perfused (1–2 mL/min) with oxygenated ACSF (in the absence of kynurenic acid). Patch micropipettes pulled from borosilicate glass capillaries (3–5 MΩ) were filled with 8 μL of autoclaved reverse transcription polymerase chain reaction (RT-PCR) internal solution (in mM): 144 K-gluconate, 3 $MgCl_2$, 0.5 ethylene glycol tetraacetic acid, 10 4-(2-hydroxyethyl)-1-piperazineethanesulfonic acid (pH 7.2, 285/295 mOsm), and 3 mg/mL biocytin for intracellular labeling. Neurons were visualized in the slice using infrared transmitted light with Dodt gradient contrast optics or epifluorescence illumination, using a Zeiss (Axioskop 2FS) microscope equipped with a ×40 water-immersion objective. Images were captured with CoolSnap HQ2 CCD camera (Photometrics) controlled by Image-Pro 5.1 software (Media Cybernetics Inc., San Diego, CA). Just before breaking the seal, GFP expression in the targeted cell was rechecked by fluorescence detection. Whole-cell recordings in current-clamp mode were performed at room temperature using a patch-clamp amplifier (Multiclamp 200B, Molecular Devices). Data were filtered at 5 kHz and digitized at 50 kHz using an acquisition board (Digidata 1322A, Molecular Devices) attached to a computer running pCLAMP 9.2 software package (Molecular Devices). All membrane potentials were not corrected for liquid junction potential.

For each recorded neuron, 28 electrophysiological parameters were quantified using custom written routines running within IgorPro (Wavemetrics). The detailed procedures are described in the Supplementary Methods S1.

Single-Cell Reverse Transcription Polymerase Chain Reaction (scRT-PCR)

At the end of the recording, the cell's cytoplasm was aspirated into the recording pipette while maintaining the tight seal. Then, the pipette was removed delicately to allow outside-out patch formation. Next the content of the pipette was expelled into a test tube, and reverse transcription (RT) was performed in a final volume of 10 μL as described previously (Lambolez et al. 1992). The scRT-PCR protocol was designed to detect simultaneously the expression of the 2 isoforms of glutamic acid decarboxylase (*GAD65* and *GAD67*), 3 genes encoding for calcium-binding proteins: calbindin D28k (CB), CR, and Parv, 3 neuropeptides NPY, SOM, and VIP, 2 transcription factors (Lhx6 and Nr2F2), and the protein reelin implicated in neuronal migration and morphology (Chameau et al. 2009). The next 2 steps of PCR were performed essentially as described previously (Ruano et al. 1995). The cDNAs present in 10 μL of the RT reaction were first simultaneously amplified by using all of the primer pairs described in Supplementary Table S1 (for

each primer pair, the sense and antisense primers were positioned on 2 different exons). GoTaq polymerase (2.5 U; Promega, Madison, United States) and 20 pmol of each primer were added to the buffer supplied by the manufacturer (final volume, 100 μL), and 21 cycles (94 °C for 30 s, 60 °C for 30 s, and 72 °C for 35 s) of PCR were run. Second rounds of amplification were performed using 2 μL of the first PCR product as template. In this second round, each cDNA was amplified individually with a second primer pair internal to the pair used in the first PCR, excepted for *Nr2F2* (nested primers, see Supplementary Table S1). Thirty-five PCR cycles were performed as described earlier (Cauli et al. 1997). Then, 10 μL of each individual PCR product were run on a 2% agarose gel using 100-bp ladders (Promega) as molecular weight marker and stained with ethidium bromide. All the transcripts were detected from 500 pg of neocortical RNA using this protocol (data not shown). The sizes of the PCR-generated fragments were as predicted by the mRNA sequences (see Supplementary Table S1).

Intracellular Labeling and Morphological Reconstructions

Slices containing recorded neurons filled with biocytin were fixed overnight at 4 °C in 4% PFA. The morphology of the recorded neurons was investigated by histochemical labeling of intracellular biocytin with diaminobenzidine (DAB) by using the ABC elite kit (Vector Laboratories, Burlingame, CA). After blocking endogenous peroxidase with 0.3% H_2O_2 in PB 0,1 M for 15–30 min, slices were rinsed in PB (4× 10 min), permeabilized in 2% Triton X-100 in PBS for 1 h, and incubated in AB diluted 1:200 in PBS and 1% Triton X-100 for 2 h. Slices were then washed in PBS (6× 10 min). For the visualization of the stain, the sections were incubated with the DAB reagent for ABC (elite kit, Vector) containing 0.05% DAB and 0.01% H_2O_2 in PBS. The reaction was monitored under a dissecting microscope and stopped by rinsing in PBS (4× 10 min) when the cell body and dendritic processes were clearly visible. The slices were then mounted in 50%PBS–50%glycerol, coverslipped, and sealed with nail polish. Biocytin-filled neurons were visualized, traced, and digitally reconstructed using the Neurolucida software (MicroBrightField, Bioscience Europe, Magdeburg, Germany) with a ×100 oil-immersion objective (Leica). The morphological parameters, quantified as mean ± standard deviation (SD) were compared for significance using Student's test. The average tortuosity of the neurons was calculated as the ratio between the distance along a process over the straight line distance, the smallest tortuosity possible being 1 for a straight path. The spatial distribution of the dendritic processes from the centroid of the cell body was studied using Wedge analysis. For this purpose, the *xy* plane was divided into 12 equiangular wedges. The total dendritic length in each wedge was then quantified (taking into account the *z* information) and displayed as a round directional histogram. The total length over all wedges corresponds to the total length of the neuronal dendritic arborization. Finally, in order to quantify the orientation of the analyzed neurons, the total dendritic length contained in the 4 most horizontally oriented wedges was divided by the length enclosed in the 4 most vertically oriented wedges. This ratio, called here "equipolarity," would be equal to 1 for a perfectly radially oriented dendritic arbor and decreases with more vertically oriented processes.

Electrophysiological Statistical Analysis

All data are presented as mean ± SD unless otherwise stated. Mann–Whitney *U* test was employed to compare electrophysiological properties between cell types. *P* values of ≤ 0.05 were considered statistically significant. To classify 5-HT_{3A}-expressing neocortical neurons sampled without a priori knowledge, unsupervised clustering was performed using 28 electrophysiological parameters (see Supplementary Methods S1) and the laminar location determined by infrared videomicroscopy. For neurons located at the border of layers I–II and II–III, the laminar location was digitized by 1.5 and 2.5, respectively. After standardizing the data, cluster analysis was performed using squared Euclidean distances and Ward's method linkage rules (Ward 1963). Ward's clustering method has been used successfully by previous studies to define neuronal classes based on multiple electrophysiological, molecular, and/or morphological features (Tamas et al. 1997; Cauli et al. 2000; Karube et al. 2004; Dumitriu et al. 2006; Gallopin et al. 2006; Halabisky et al. 2006; Dávid et al. 2007; Andjelic et al. 2008; Helmstaedter et al. 2009; Karagiannis et al. 2009). Thorndike analysis of the critical threshold was conducted to suggest the likely number of different clusters in the data set (Thorndike 1953). Descriptive statistics and cluster analysis were calculated with Statistica v 6.0 (Statsoft, Tulsa, OK).

Birth Dating In Vivo

Pregnant females of the Swiss genetic background received a single 5-bromo-2-deoxyuridine (BrdU) injection (IP, 50 mg/kg; in 0.9% NaCl) at gestational days E11.5, E12.5, E13.5, E14.5, E15.5, or E16.5. Animals, aged P25, were anesthetized as described above and perfused transcardially with 4% PFA. Cryosections (17 μm thick) were first processed for in situ hybridization to reveal 5-HT_{3A} mRNA transcripts and then processed for immunocytochemistry to detect BrdU. Nonradioactive in situ hybridization was performed as described in Schaeren-Wiemers and Gerfin-Moser (1993) (products were purchased from Roche Diagnostics). Sense probes were used as control and did not show any labeling. Subsequently, sections were treated with 2 N HCl for 45 min, rinsed in 0.1 M PBS, pH 7.4, incubated during 1 h in PBS supplemented by normal goat serum (10%) and incubated overnight with anti-BrdU (1:100, Progen, GmbH, Germany) in PBS. After washing, sections were incubated 2 h in Alexa Fluor 488 goat antimouse antibody (1:200, Invitrogen) and were mounted in Vectashield containing Dapi. To estimate the number of BrdU-labeled cells among the 5-HT_{3A}-expressing population, a least 3 litters were analyzed per time point, and at least 2 animals per litter were processed for histology. For each anatomical area selected, 5 adjacent sections were analyzed per case. On each section, the number of 5-HT_{3A}+ neurons heavily labeled for BrdU (defined as having >50% of the nucleus immunolabeled; Gillies and Price 1993) was estimated using a ×40 objective. The number of double-labeled cells was expressed as percentage of cells double labeled over the 5-HT_{3A}+ population. In the primary somatosensory cortex, the total number of cells per radial sector of (700-μm width) was pulled to produce the graphs.

In Utero Cells Transplantation

Homochronic transplantations were performed using E13/E13.5 and E14/E14.5 donor and host embryos. Donor embryos were collected into cold PBS following cervical dislocation of the pregnant mouse. Embryonic heads were dissected into cold L15 medium and embedded in 3% low-melting-point agarose (Sigma) in L15 medium. From these blocks, 270–300-μm-thick coronal sections were obtained using a Leica vibroslicer (Leica VTS1000) and were collected into cold L15 medium. CGE and AEP/preoptic (AEP/Po) explants were dissected out of the sections, collected into L15 medium, and kept on ice until transplantation. CGE or AEP/Po were mechanically dissociated prior transplantation. In addition, some experiments were performed using 5-HT_{3A}:GFP+ cells sorted by flow cytometry (see Supplementary Method S2). For transplantation, time mate pregnant OF1 mice (Charles River) were anaesthetized with Xylazine–Ketamine (1 mg/kg/IP; 10 mg/kg/IP, in sterile saline solution). Uterine horns were exposed, and each embryo was manipulated under the uterine wall until position of the lateral ventricle was discernable. A glass micropipette (50 μm) containing an average of 5×10^4–10^5 cells in L15 stained with blue trypan (in 1 μL of solution) was introduced through the placenta in the ventricle (lateral or third) of each embryo. Cell transfer was achieved using mouth-control tubing attached to the pipette. The procedure was repeated for each embryo except for the most proximal and distal embryos. Injections were performed using E13/E13.5 5-HT_{3A}:GFP (CGE: $n = 6$ litters, $n = 18$ hosts; AEP/Po: $n = 5$ litters, $n = 20$ hosts) or using E14/E14.5 5-HT_{3A}:GFP donors (for cell suspension: CGE: $n = 10$ litters, $n = 43$ hosts; AEP $n = 12$ litters, $n = 40$ hosts, and for FACsorted cells: $n = 2$ litters, $n = 5$ hosts). After surgical recovery, animals were returned to their cages, and pups were reared until postnatal days 16–25 (P16–P25). Animals were processed as described above.

The distribution of 5-HT_{3A}:GFP+ grafted cells was determined on coronal sections counterstained with bis-benzimide. Quantification of GFP+ cells in the somatosensory cortex was carried out under a fluorescent microscope (Leica, DMR) using a 250 000-μm^2 area under a ×20 objective lens or a 66 000-μm^2 area under a ×40 objective lens. The laminar distribution of GFP+ cells was quantified at the level of the primary somatosensory area, in 500-μm-wide cortical strips (data obtained from 3 adjacent sections of at least 7 animals and expressed as

mean ± standard error of the mean). The proportion of GFP+ grafted cells labeled for Parv, SOM, CR, VIP, or NPY was estimated in a cortical strip (700-μm width) in the primary somatosensory area and was expressed as percentage of double-labeled cells over the GFP+ population (data obtained from 3 adjacent sections of at least 12 animals from 5 different experiments).

Results

Distribution and Neurochemical Phenotype of Telencephalic 5-HT$_{3A}$-Expressing Neurons in Adult Wild-Type and Transgenic 5-HT$_{3A}$:GFP Mice

The 5-HT$_{3A}$ receptor expression pattern in the adult wild-type mice telencephalon was first studied by in situ hybridization (Fig. 1*A–C*). The distribution of 5-HT$_{3A}$ mRNA transcripts closely mirrored that previously reported in the rat (Tecott et al. 1993; Morales and Bloom 1997). The 5-HT$_{3A}$ mRNA was detected in the cortex, olfactory bulb, hippocampal formation, amygdaloid complex, septum, and hypothalamus. Within the neocortex, 5-HT$_{3A}$ mRNA-expressing cells were preferentially located in supragranular layers I–III and to a lesser extent in infragranular layers V–VI (Fig. 1*A–C*). This pattern of expression was observed from the frontal to the occipital regions of the neocortex. The detailed laminar distribution of 5-HT$_{3A}$-expressing cells within the primary somatosensory cortex is illustrated in Figure 1*B*.

To further study 5-HT$_{3A}$-expressing neurons, we decided to use BAC transgenic mice where the 5-HT$_{3A}$ expression is accurately reported by GFP (Heintz 2001). Two 5-HT$_{3A}$:GFP BAC mouse lines were tested of which 1 was generated in H.

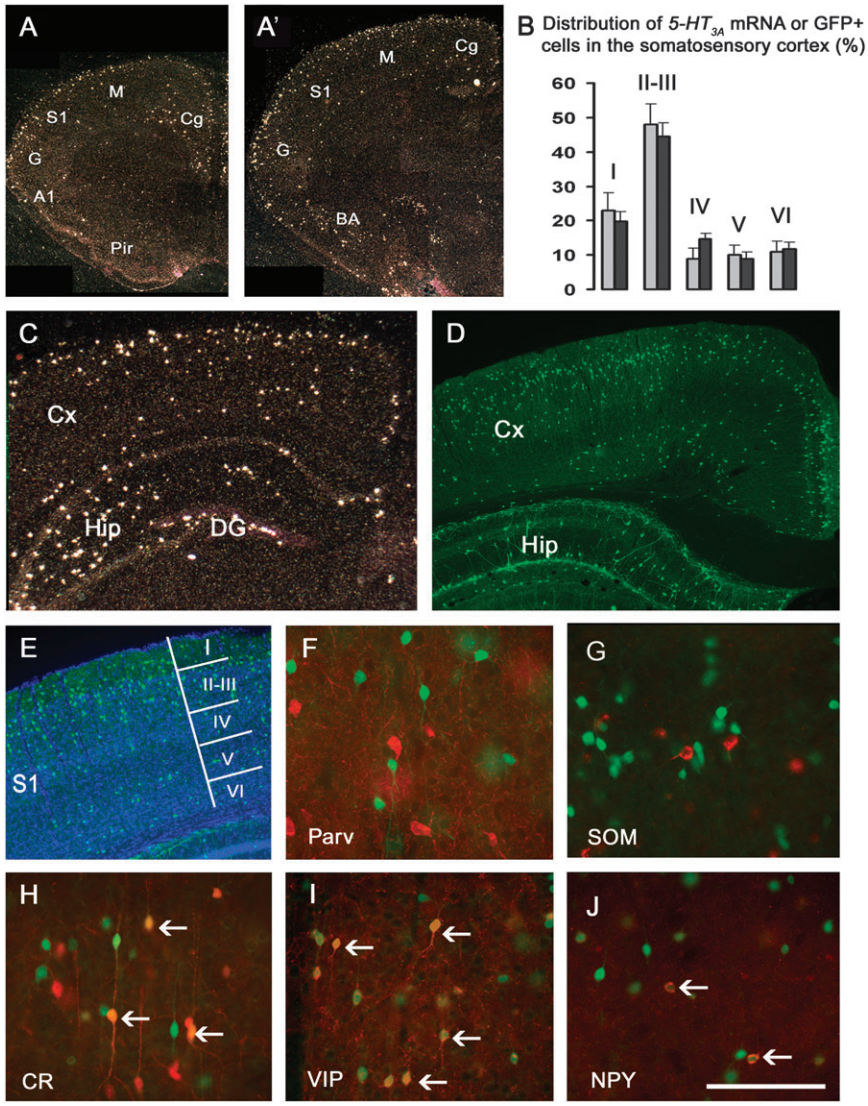

Figure 1. Expression of 5-HT3A in the adult telencephalon. (*A*, *A′*, *C*) Coronal sections from an adult wild-type mouse showing the distribution of 5-HT$_{3A}$ transcripts. (*B*) Graph showing the density of both 5-HT$_{3A}$ mRNA-expressing cells from adult wild-type animals (gray bars) and 5-HT$_{3A}$:GFP+ cells from transgenic 5-HT$_{3A}$:GFP mice (black bars) in the different layers of the somatosensory cortex. Data are means ± standard error of the mean (SEM). (*C*,*D*) Sections from identical stereotaxic levels showing "a similar location of both 5-HT$_{3A}$ mRNA-expressing cells from a wild type" mouse (*C*) and GFP fluorescent cells from a 5-HT$_{3A}$:GFP mouse (*D*). (*E*) Coronal section of a 5-HT$_{3A}$:GFP mouse counterstained with Dapi (blue) showing the preferential location of 5-HT$_{3A}$-expressing cells in supragranular layers. Cortical layers are indicated. (*F–J*) Expression of 5-HT$_{3A}$:GFP (green) is restricted to subpopulations of interneurons (red). (*F*,*G*) Overlays showing the lack of Parv (*F*) or SOM (*G*) expression in GFP+ cells. (*H–J*) Overlays showing the colocalization of GFP with CR (*H*), VIP (*I*), or NPY (*J*). A1, agranular insular cortex; BA, basolateral amygdaloid nucleus; Cg, cingulate cortex area; Ctx, cerebral cortex; G, gustatory cortex area; Hip, hippocampus; M, motor cortex area; Pir, piriform cortex; S1, somatosensory cortex area; Scale bar: (*A–A′*) 1 mm; (*C*,*D*) 700 μm; (*E*) 500 μm; and (*F–J*) 100 μm.

Monyer's laboratory (Inta et al. 2008) and the other was provided by GENSAT (see animals in the Materials and Methods section). Both mouse lines showed a similar distribution of cortical 5-HT_{3A}:GFP+ neurons, which also mirrored the expression pattern of 5-HT_{3A} transcripts observed in wild-type animals (Fig. 1*C–E*). The laminar density of both GFP immunoreactive cells from 5-HT_{3A}:GFP transgenic mice and 5-HT_{3A} mRNA-expressing cells from wild-type animals, quantified within the primary somatosensory cortex indeed revealed similar distribution profiles (Fig. 1*B*). In situ hybridization performed on 5-HT_{3A}:GFP+ animals confirmed the expression of 5-HT_{3A} mRNA in GFP immunoreactive cells (Supplementary Fig. S1) and Western blot analysis showed that GFP expression does not alter 5-HT_{3A} protein synthesis (Supplementary Fig. S2).

The observation of 5-HT_{3A}:GFP+ cells clearly revealed a nonpyramidal morphology, suggesting that the 5-HT_{3A} receptor is expressed by a subpopulation of GABAergic INs in the mouse neocortex, similarly to what has been observed in the rat (Morales and Bloom 1997; Ferezou et al. 2002; see also Jakab and Goldman-Rakic 2000 for comparison with primate cerebral cortex). Hence, we next performed immunohistochemical analyses to assess the expression of neurochemical markers usually used to classify INs subtypes such as CR, VIP, Parv, SOM, and NPY (Kawaguchi and Kondo 2002). We found that in all telencephalic regions, 5-HT_{3A}:GFP+ INs did not express Parv or SOM (Fig. 1*F,G*) whereas CR, VIP, and NPY were frequently detected (Fig. 1*H–J*). Within the primary somatosensory cortex, the proportion of cells in which GFP colocalized with 1 of the 3 markers was layer dependent (see Supplementary Table S2). Indeed, VIP/GFP+ and CR/GFP+ INs were preferentially located in layers II–III whereas NPY/GFP+ INs were distributed in all cortical layers.

These results therefore indicate that the 5-HT_{3A} expression is likely to characterize specific subtypes of cortical interneurons.

Characterization and Classification of Cortical 5-HT_{3A}-Expressing Interneurons in the Juvenile Somatosensory Cortex

To further describe the electrophysiological, molecular, and morphological properties of 5-HT_{3A}-expressing cortical interneurons, a sample of GFP-positive cells from layer I ($n = 12$) and II–III ($n = 41$) was analyzed by combining patch-clamp recordings, scRT-PCR and biocytin labeling on somatosensory cortex slices from 5-HT_{3A}:GFP mice (P14–P17).

The scRT-PCR protocol was designed to detect mRNAs encoding for 8 molecular markers commonly used to define subpopulations of cortical neurons: GAD65, GAD67, CB, Parv, CR, NPY, VIP, and SOM. In addition, we assessed the expression of 3 developmental markers known to be involved in the maturation of neocortical neurons: Reelin (Chameau et al. 2009), Lhx6 (Liodis et al. 2007), and Nr2F2 (Kanatani et al. 2008). In this report, cells positive for GAD65 and/or GAD67 are denoted as GAD positive. Only cells expressing *GAD* and at least 1 gene encoding for 1 neuropeptide or 1 calcium-binding protein were analyzed.

Neurons expressing 5-HT_{3A} were classified using unsupervised cluster analyses based on their laminar location and 28 electrophysiological parameters (see Supplementary Methods S1) adopting Petilla terminology (Ascoli et al. 2008; Karagiannis et al. 2009). On the basis of the Thorndike threshold, this multifactorial analysis segregated 5-HT_{3A}-expressing neurons into 2 clusters of cells corresponding to branches a and b in the tree diagram (Fig. 2). The molecular profile of these clusters has been established by plotting the percentage of neurons expressing given molecular markers for each group. Each cluster was then named according to its prominent characteristics: the high NPY expression level for cluster a (NPY-cluster, $n = 31$) and the large occurrence of VIP expression in cluster b (VIP-cluster, $n = 22$). Expression of *Lhx6* was almost never detected on both VIP- and NPY-cluster (0% and 6%, respectively). Indeed, *Lhx6* is known to be associated with other subtypes of interneurons expressing Parv or SOM (Liodis et al. 2007).

The laminar distribution of these interneurons appears to be different between the 2 clusters because all the cells recorded in the layer I ($n = 12$) belong to the NPY-cluster (in addition to 19 layers II–III NPY neurons), whereas all the VIP-cluster neurons were located in the layers II–III ($n = 22$). As expected by the targeting of our recordings toward GFP fluorescent neurons,

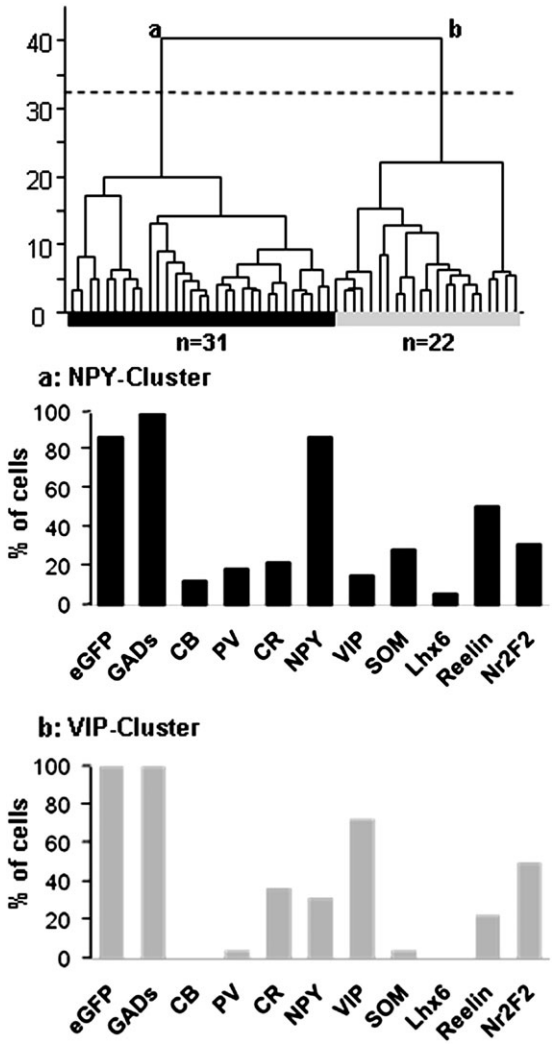

Figure 2. Unsupervised cluster analysis applied to GFP-positive neocortical neurons. The *x* axis represents individual cells, and the *y* axis represents the average within-cluster linkage distance. Distances were calculated on the basis of the laminar location of the cells, in addition to 28 electrophysiological parameters (see Supplementary Methods S1). On the basis of the Thorndike threshold (dotted line), this analysis disclosed 2 groups of cells (corresponding to branches a and b): the NPY-cluster (black) and the VIP-cluster (gray). Histograms show the distribution of molecular markers within each cluster.

eGFP mRNA was detected in a large majority of the cells (in 100% of the VIP-cluster cells and in 87% of the NPY-cluster cells). Representative examples of interneurons from each cluster are presented in Figure 3 and Supplementary Fig. S3.

The NPY-cluster of 5-HT$_{3A}$ Interneurons

The major molecular characteristics of neurons in the NPY-cluster were the high occurrence of *NPY* (n = 27/31, 87%), *reelin* (52%), and *Nr2F2* (32%). These neurons expressed to a lower extent mRNAs for *SOM* and *CR* (29% and 23%, respectively). mRNAs for *Parv*, *VIP*, and *CB* were slightly present in this group (19%, 16%, and 13%, respectively). Neurons of the NPY-cluster were characterized by distinctive electrophysiological properties (see Supplementary Methods S1), in particular when depolarized just above the threshold of action potential generation (see example illustrated in Fig. 3*A*1). Indeed, the main electrophysiological hallmarks of this group of cells were a high rheobase, a long latency of action

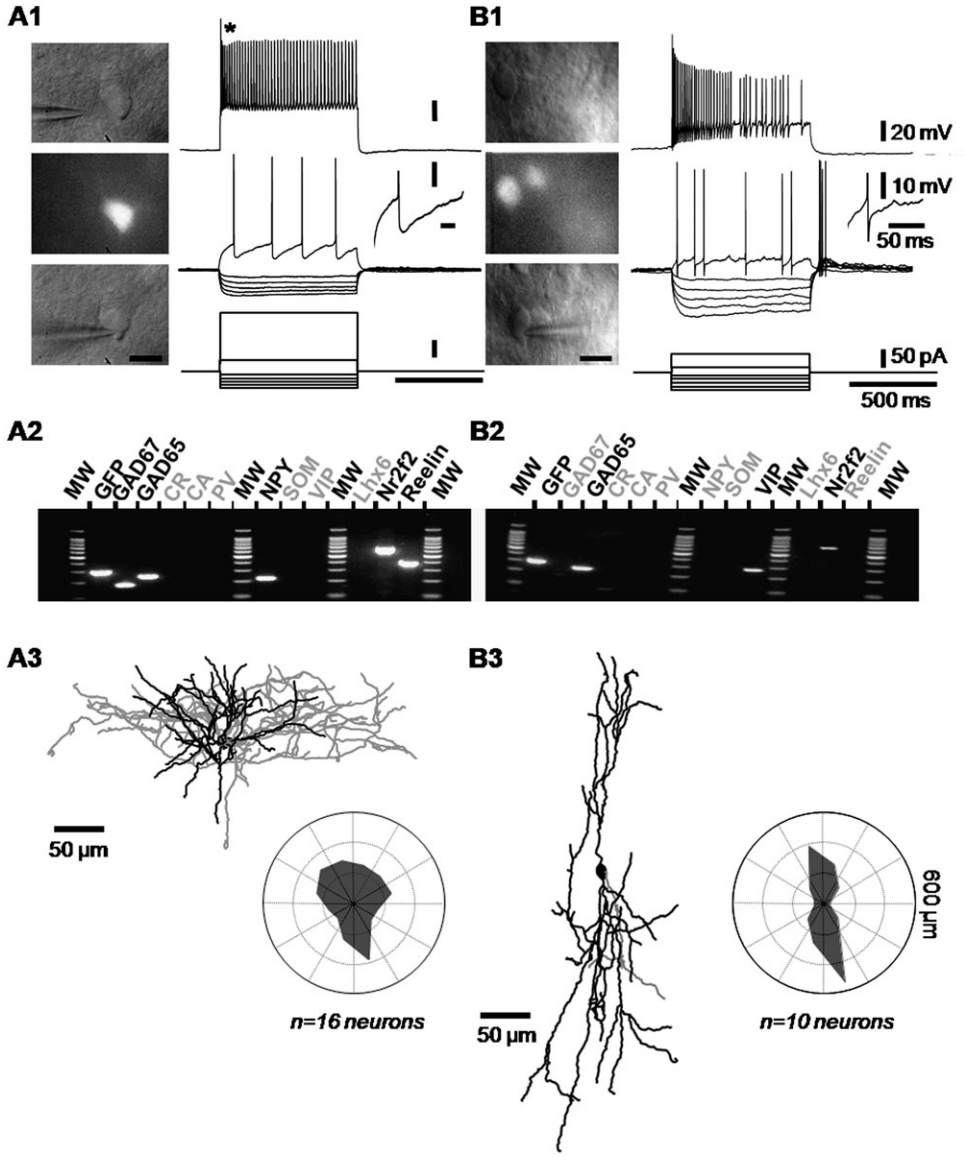

Figure 3. Electrophysiological, molecular and morphological properties of 5-HT$_{3A}$-expressing interneurons of the NPY-cluster and VIP-cluster. (*A*1) The electrophysiological behavior of a neuron belonging to the NPY-cluster was recorded using whole-cell patch-clamp recording in current-clamp mode, in response to current pulses injections (lower traces). Suprathreshold and just above the threshold responses are illustrated in the upper and medium traces, respectively. Just above threshold current induced the delayed firing of action potentials. Application of a larger depolarizing current induced a marked frequency adaptation with pronounced amplitude accommodation (upper trace, asterisk). The right inset shows the repolarization phase of the first action potential. Note the monophasic aspect of the after hyperpolarization. The Infrared and epifluorescence images of the same neuron have been taken just before the recording (top and middle panels) and during the recording (bottom panel) (scale bar 10 µm). (*A*2) Agarose gel showing the expression of *GFP*, *GAD67*, *GAD65*, *NPY*, *Nr2F2*, and *Reelin*. (*B*1) Voltage traces recorded from a VIP-cluster neuron in response to current pulses (lower traces). The right inset details the complex repolarization phase of the first action potential. On the left panels, the infrared and epifluorescence images of the same cell were taken just before and during the recording (scale bar: 10 µm). (*B*2) Agarose gel showing the expression of *GFP*, *GAD65*, *VIP*, and *Reelin*. (*A*3,*B*3) Neurolucida reconstructions of the neurons shown in (*A*1,*B*1), respectively. Axons are represented in gray, whereas somata and dendrites are illustrated in black. Cells of the NPY-cluster show characteristics of "neurogliaform" neurons: the soma of these cells is rather multipolar with smooth dendrites and the axon is densely distributed within and around the dendritic arborization (*A*3). VIP-positive cells are characterized by their bipolar, vertically oriented main dendrites and axon (*B*3). Polar histograms illustrate the results of the Wedge analysis for each cluster of cells. The dendritic arbors organization around the centroid of the cells bodies was quantified by plotting the averaged dendritic length for each equiangular wedge.

potentials discharge, a weak acceleration of their firing rate, and low minimal frequency (Table 1). These electrophysiological features indicated a slow spiking behavior near threshold. The large majority of neurons belonging to the NPY-cluster (90%) fired action potentials with monophasic after hyperpolarizations (AHPs) resulting in the absence of after depolarizing potential component (ADP). At higher stimulation intensities, these cells displayed a frequency adaptation and a pronounced amplitude accommodation.

Of the 31 recorded neurons belonging to the NPY-cluster, 16 were analyzed for their morphological properties following their histochemical staining and 3D reconstruction (see example in Fig. 3*A*3). Indeed, neurons that were not sufficiently well stained, located too deep into the slice to focus properly, or too superficial, presenting truncated processes, had to be discarded. In many cases, we had difficulties in recover the entire axonal arborisation of the reconstructed neurons. Indeed, high sc-RT-PCR efficiency requires harvesting the cytoplasm of GFP+ cells within 10 min, and this is not optimal for biocytin labeling (Karagiannis et al. 2009). We therefore focus our observations on the neuronal somatodendritic features of the interneurons. Although the NPY-cluster regrouped neurons presenting heterogeneous aspects, the most prominent traits of this group are a relatively high number of primary dendrites emerging from the soma (7.9 ± 4.5), a dendritic arborization radially organized (equipolarity = 0.98 ± 0.10, see Wedge analysis presented in Fig. 3*A*3), and a notable tortuosity of the processes (1.4 ± 0.1). In the following part of this paper, we will refer to them as NPY multipolar/neurogliaforms.

The VIP-cluster of 5-HT$_{3A}$ Interneurons

Unsupervised clustering discriminated another group of cells characterized by a high occurrence of *VIP* mRNA (n = 16/22, 73%). *CR* (36%), *NPY* (32%), and *Nr2F2* (50%) were also frequently expressed in this group whereas *CB*, *Parv*, and *SOM* mRNAs were rarely detected (Fig. 2). Neurons of the VIP-cluster exhibit 2 types of firing behavior, adapting (n = 15/22, 68%) or bursting (n = 7/22, 32%) as described previously (Cauli et al. 1997; Karagiannis et al. 2009). In comparison with the NPY-cluster neurons, neurons of this cluster exhibited more depolarized resting membrane potential and lower rheobase, suggesting that they should be electrically more excitable (Table 1). Cells of the VIP-cluster exhibited the highest input resistance and membrane time constant of our sample. They fired action potentials with larger spike amplitude and shorter spike latency, exhibiting in some cases a biphasic repolarization phase. Indeed, the first 2 action potentials of adapting VIP were followed by a first AHP component, an ADP, and a late AHP component (n = 8/15). However, this repolarization behavior was almost never observed in bursting-VIP cells (n = 2/7).

Of the 22 recorded neurons belonging to the VIP-cluster, 10 were analyzed for their somatodendritic morphological properties (see example in Fig. 3*B*3). These interneurons presented less primary dendrites emerging from the soma than NPY-cluster neurons (4.5 ± 2.1 vs. 7.9 ± 4.5, respectively), although this difference was not significant. The most striking particularity of these cells was the bipolar organization of their dendritic tree (equipolarity = 0.18 ± 0.25, see the wedge diagram in Fig. 3*B*3). Finally, the dendritic processes of the VIP-cluster neurons are less tortuous than those of the NPY-cluster neurons (1.25 ± 0.11 vs. 1.39 ± 0.13, P = 0.01).

Birth-Dating Analysis of Cortical 5-HT$_{3A}$-Expressing Interneurons

Having characterized 2 types of cortical interneurons expressing the 5-HT$_{3A}$ subunit, we next investigated their date of genesis. Although Inta et al. (2008) have reported that

Table 1
Electrophysiological properties of 5-HT$_{3A}$-expressing neocortical interneurons

Electrophysiological parameters	VIP-cluster (n = 22)	NPY-cluster (n = 31)	Electrophysiological parameters	VIP-cluster (n = 22)	NPY-cluster (n = 31)
(1) Resting potential (mV)	−55.98 ± 3.92	−60.5 ± 5.59	(15) First spike amplitude (mV)	83.82 ± 9.8	75.1 ± 9.72
	VIP-cluster << VIP-cluster			NPY-cluster << VIP-cluster	
(2) Input resistance (MΩ)	761.45 ± 306.46	391.92 ± 124.15	(16) Second spike amplitude (mV)	78.80 ± 8.86	70.6 ± 10.6
	NPY-cluster <<< VIP-cluster			NPY-cluster < VIP-cluster	
(3) Time constant (ms)	40.61 ± 19.53	25.65 ± 12.09	(17) First spike duration (ms)	0.95 ± 0.37	1.8 ± 0.53
	NPY-cluster << VIP-cluster			VIP-cluster <<< NPY-cluster	
(4) Membrane capacitance (pF)	56.94 ± 25.39	66.20 ± 25.52	(18) Second spike duration (ms)	0.99 ± 0.38	2.00 ± 0.52
	VIP-cluster — NPY-cluster			VIP-cluster < < < NPY-cluster	
(5) Sag index (%)	12.09 ± 7.83	5.84 ± 6.02	(19) Amplitude reduction (%)	5.78 ± 5.1	5.99 ± 6.98
	NPY-cluster << VIP-cluster			VIP-cluster — NPY-cluster	
(6) Rheobase (pA)	17.72 ± 9.22	64.83 ± 71.36	(20) Duration increase (%)	4.54 ± 2.69	11.43 ± 15.53
	VIP-cluster << NPY-cluster			VIP-cluster << NPY-cluster	
(7) First spike latency (ms)	133.00 ± 147.21	243.01 ± 235.14	(21) First spike, AHP max (mV)	−16.07 ± 4.1	−12.10 ± 3.89
	VIP-cluster — NPY-cluster			VIP-cluster << NPY-cluster	
(8) Adaptation (Hz/s)	−12.12 ± 21.59	4.1 ± 24.28	(22) Second spike, AHP max (mV)	−17.58 ± 3.47	−14.30 ± 3.25
	VIP-cluster << NPY-cluster			VIP-cluster << NPY-cluster	
(9) Minimal steady state frequency (Hz)	14.53 ± 11.21	7.42 ± 5.17	(23) First spike, AHP max latency (ms)	5.82 ± 1.40	15.2 ± 6.88
	NPY-cluster << VIP-cluster			VIP-cluster <<< NPY-cluster	
(10) Amplitude accommodation (mV)	0.88 ± 2.18	3.11 ± 0.83	(24) Second spike, AHP max latency (ms)	10.11 ± 14.63	16.3 ± 6.79
	VIP-cluster << NPY-cluster			NPY-cluster < < < VIP-cluster	
(11) Amplitude of early adaptation (Hz)	57.85 ± 34.81	46.73 ± 27.15	(25) First spike ADP (mV)	1.02 ± 1.72	0.1 ± 0.23
	VIP-cluster — NPY-cluster			VIP-cluster < NPY-cluster	
(12) Time constant of early adaptation (ms)	23.93 ± 9.21	33.92 ± 40.48	(26) Second spike ADP (mV)	0.80 ± 1.28	0.0 ± 0.10
	VIP-cluster — NPY-cluster			VIP-cluster < NPY-cluster	
(13) Late adaptation (Hz/s)	−26.99 ± 18.79	−10.08 ± 17.64	(27) First spike ADP latency (ms)	1.89 ± 2.8	0.2 ± 0.85
	VIP-cluster << NPY-cluster			NPY-cluster < VIP-cluster	
(14) Maximal steady state frequency (Hz)	75.11 ± 21.36	46.76 ± 17.58	(28) Second spike ADP latency (ms)	1.67 ± 2.56	0.1 ± 0.56
	NPY-cluster <<< VIP-cluster			NPY-cluster < VIP-cluster	

telencephalic 5-HT_{3A}:GFP+ cells can be generated as early as embryonic day E12.5, we wanted to determine more specifically the birth date of neocortical 5-HT_{3A}-expressing neurons. With this aim, we used BrdU labeling combined with 5-HT_{3A} mRNA detection. Wild-type mice received a single injection of BrdU at a given stage (between E11.5 and E16.5), a minimum of 3 litters per time point were subsequently analyzed at P25 and at least 2 animals per litter were processed for histology. These experiments revealed that 5-HT_{3A}-expressing neurons are generated at distinct embryonic stages according to their telencephalic region of destination.

A large proportion of 5-HT_{3A}-expressing neurons populating the neocortex were generated over a narrow period, between E13.5 and E14.5 (Fig. *4A–C,F,H–K*). In contrast, 5-HT_{3A}-expressing neurons of the cingulate and retrosplenial cortices were generated 1 day earlier compared with those located in the neocortex at similar stereotaxic levels (Fig. *4D,I–K*). Within the hippocampal formation, 5-HT_{3A} interneurons were mainly generated over the E12.5–E13.5 period (Fig. *4E,G,J,K*), before the genesis of glutamatergic neurons (Soriano et al. 1989). Birth-dating analysis of 5-HT_{3A}-expressing neurons in the piriform cortex was more heterogeneous than in other regions of the hippocampal formation, extending from E12.5 to E16.5 (Fig. *4I,J*). Finally, 5-HT_{3A} neurons located in the amygdala were generated between E12.5 and E14.5, with a peak of genesis at E13.5 (Fig. *4J–K*).

The birth of 5-HT_{3A}-expressing neurons therefore occurs within a variety of embryonic time windows according to their destination, with a specific peak of genesis between E13.5 and E14.5 for the 5-HT_{3A} neocortical interneurons.

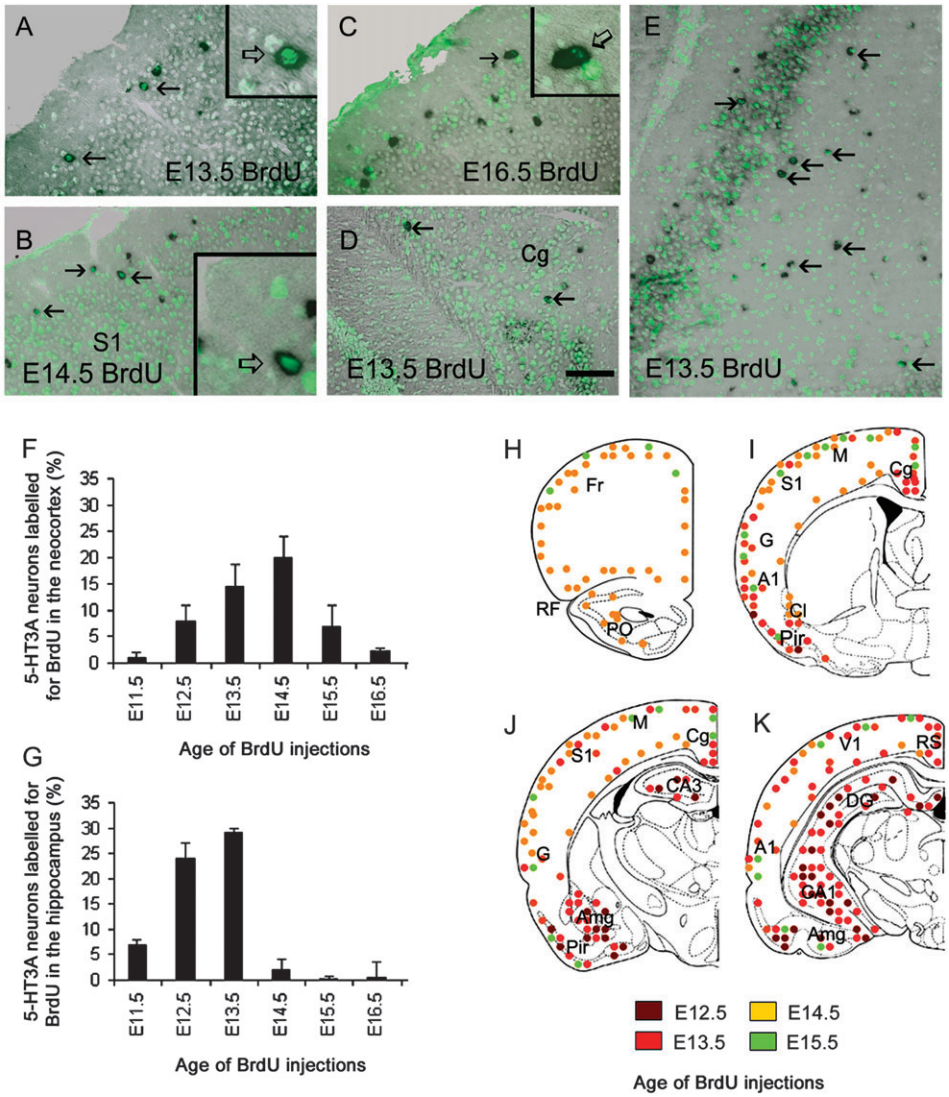

Figure 4. Birth-dating of telencephalic 5-HT3A interneurons. (*A–E*) Simultaneous detection of 5-HT_{3A} transcripts (black) and BrdU (green) in coronal sections at the level of the cerebral cortex (*A–C*), the cingulated cortex (*D*) and the hippocampus (*E*) in P25 wild-type mice. Age of pulse injection is indicated on the images. (*A–C*) Coronal sections taken at the level of the primary somatosensory cortex showing double-labeled cells in the supragranular layers (arrows). (*D*) Coronal section taken at the level of the cingulate cortex. (*F,G*) Histograms showing the percentage of 5-HT3A-expressing cells labeled for BrdU after a pulse injection at a given age, quantified in the neocortex (*F*) and the hippocampus (*G*). Note that the peak of genesis of cortical 5-HT_{3A}-expressing cells takes place around E14.5. Data are represented as mean ± SEM (percentage of double-labeled cells over the 5-HT_{3A}-postive cells). (*H–K*) Drawings showing the location and date of genesis of 5-HT_{3A}-expressing cells. Drawings are presented from rostral (*H*) to caudal (*K*). A1, auditory cortex; Amg, amygdala; CA1-3, field CA1-3 of the hippocampus; Cl, claustrum; Cg, cingulate cortex area; DG, dentate gyrus; Fr, Frontal cortex area G, gustatory cortex area; M, motor cortex area; Pir, piriform cortex; PO, primary olfactory cortex; RF, Rhinal fissure; RS, retrosplenial cortex; S1, somatosensory cortex area; V1, visual cortex area. Scale bar: (*A–D*) 200 μm; (*E*) 250 μm.

Localization of 5-HT$_{3A}$-Expressing Neurons during Mouse Embryogenesis

Johnson and Heinemann (1995) have described a very early expression of 5-HT$_{3A}$ mRNA in the basal telencephalon, a region well known to give rise to cortical interneurons (Marín and Rubenstein 2001). Having determined precisely the peak of genesis of cortical 5-HT$_{3A}$-expressing interneurons, we next analyzed the specific 5-HT$_{3A}$ distribution at this embryonic stage (E13.5–E14.5). In this aim, we used both GFP immunodetection in 5-HT$_{3A}$:GFP mice and 5-HT$_{3A}$ mRNA detection in wild-type animals (Fig. 5).

We found a good correlation between regions of high 5-HT$_{3A}$ mRNA expression (Fig. 5*C,G*) and high GFP-immunoreactivity (Fig. 5*D,H*). At E13.5, expression was highest in the AEP/Preoptic (AEP/Po) region, whereas discrete labeling was also observed in the CGE (data not shown). At E14.5, 5-HT$_{3A}$ expression was high both in AEP (Fig. 5*A,C–D*) and CGE (Fig. 5*E,G–H*) 2 regions included in territories expressing the transcription factor *Dlx1/2* that is required for interneuron specification (Anderson et al. 1999).

Within the CGE, the expression of the differentiation marker class III β-tubulin (tuj-1; Menezes and Luskin 1994) in GFP+ neurons reveals their postmitotic state (Fig. 5*I–L*).

Both MGE and LGE contained only scattered GFP+ neurons (Fig. 3*M*), presumably corresponding to interneurons that will populate the olfactory bulb (LGE) and interneurons passing through these structures (Marín and Rubenstein 2001). We observed that all GFP immunoreactive cells (E14.5, n = 9 embryos) migrating tangentially along the intermediate zone were also immunoreactive for GABA (Fig. 5*H,N–Q*). However, GFP was only found in a subset of GABA immunoreactive cells in the low intermediate zone (LIZ, Fig. 5*N-Q*) ~42% (rostral level) and ~67% (caudal level; Fig.5*H,N*).

Contribution of CGE and AEP/Po in the Genesis of Cortical 5-HT$_{3A}$-Expressing Interneurons

To determine the relative contribution of AEP/Po and CGE in the genesis of cortical 5-HT$_{3A}$-expressing interneurons homochronic in vivo grafts of AEP/Po- and CGE-derived postmitotic neurons from 5-HT$_{3A}$:GFP embryos into wild-type host embryos were performed at the peak of genesis of cortical 5-HT$_{3A}$ interneurons.

Figure 6*A* shows the territories dissected and used for donor tissues. Subsequently, the positions of 5-HT$_{3A}$:GFP+ grafted cells were analyzed in host mice (P19–P25). In Figure 6*B* schematic drawings of coronal sections of grafted animals indicate the location of 5-HT$_{3A}$:GFP+ grafted cells. Both AEP and CGE contributed to several telencephalic structures; however, only CGE-derived cells populated the neocortex.

Contribution of AEP/Po

In utero grafts of E13/E13.5 AEP/Po-derived cells demonstrated that 5-HT$_{3A}$:GFP+ grafted cells contribute to populate the hippocampal formation as grafted cells were mostly found in the dentate gyrus (Fig. 6*B*). 5-HT$_{3A}$:GFP+ cells grafted from the caudal part of the AEP at E14/E14.5 mainly populated the amygdala (basolateral and lateral nuclei), the endopiriform nucleus and the claustrum. Grafted cells from the rostral part of the AEP gave rise to rare cells located in the deep cortical layers of the retrosplenial and motor cortices (Fig. 6*B*). These results demonstrate that at the peak of genesis of neocortical 5-HT$_{3A}$-expressing interneurons (E14.5, Fig. 4*F*), cells generated in AEP/Po do not contribute to the genesis of cortical 5-HT$_{3A}$ interneurons.

Contribution of CGE

E13/E13.5 and E14/E14.5 CGE-derived cells contribute to populate the neocortex (Figs. 6 and 7), in addition to several limbic structures, including the bed nucleus of the stria terminalis, the hippocampus, and several nuclei of the amygdala (Fig. 6*B*). Within the hippocampal formation, the majority of grafted cells were located in CA3 and CA1, whereas fewer cells were found in the hilus and the dentate gyrus (Fig. 6*B*). Within the amygdaloid complex, grafted cells were found in the basolateral, the lateral and the corticoamygdaloid nuclei (Fig. 6*B*). E14/E14.5 CGE-derived cells were more often found in the neocortex and amygdala compared with E13/E13.5 CGE-derived cells that were mainly populating hippocampal structures (Fig. 6*B*).

Interestingly, homotopic and homochronic in vitro grafts of E14.5 GFP+ donor cells derived from CGE into wild-type slices clearly show that GFP+ cells migrate toward the amygdala and the cortex following several migratory routes, along the marginal zone and along the subventricular zone (Supplementary Fig. S4).

Most fluorescent grafted cells that were observed in the neocortex were located in supragranular layers I–III (Fig. 7*B–F*). Note that similar results were obtained in animals receiving 5-HT$_{3A}$:GFP+ cells freshly dissected or sorted by flow cytometry (Fig. 7*C–D*). Within the cortical layers II–III, some of these cells displayed characteristic bipolar/double bouquet morphologies and therefore presumably belong to the VIP-cluster of 5-HT$_{3A}$-expressing interneurons (Fig. 7*E*). We also found multipolar/neurogliaform cells presumably belonging to the NPY-cluster. These cells displayed complex morphologies and were distributed throughout the layers I and II–III (Fig. 7*F*). To determine the phenotype of grafted cells, we used several immunohistochemical markers commonly used to discriminate different interneurons classes. In all telencephalic regions, grafted cells displayed the same phenotype as those observed in 5-HT$_{3A}$:GFP animals. Grafted cells never displayed Parv or SOM immunoreactivity, but expressed CR, VIP, and NPY (Fig. 7*G–O,P*).

Discussion

In this study, we show that 5-HT$_{3A}$ is protractedly expressed from early postmitotic to adult stages by selective subpopulations of mouse neocortical interneurons. Although the functional role of the 5-HT$_{3A}$ subunit during early developmental stages is yet unresolved (but see also Riccio et al. 2008), its protracted expression enabled us to follow the development of neocortical 5-HT$_{3A}$+ interneurons. Various techniques including homochronic in utero grafts performed at the peak of genesis of cortical 5-HT$_{3A}$+ interneurons revealed that these neurons are mainly generated in the CGE. We further demonstrate that grafted interneurons retain their specific neurochemical phenotype, distribution, and functional properties after grafting, as previously described for different subpopulation of neocortical interneurons (Nery et al. 2002; Butt et al. 2005). The characterization of mature neocortical 5-HT$_{3A}$-expressing interneurons from 5-HT$_{3A}$:GFP mice shows that 5-HT$_{3A}$ is expressed by VIP-expressing bipolar/bitufted interneurons and NPY-expressing interneurons displaying more complex dendritic

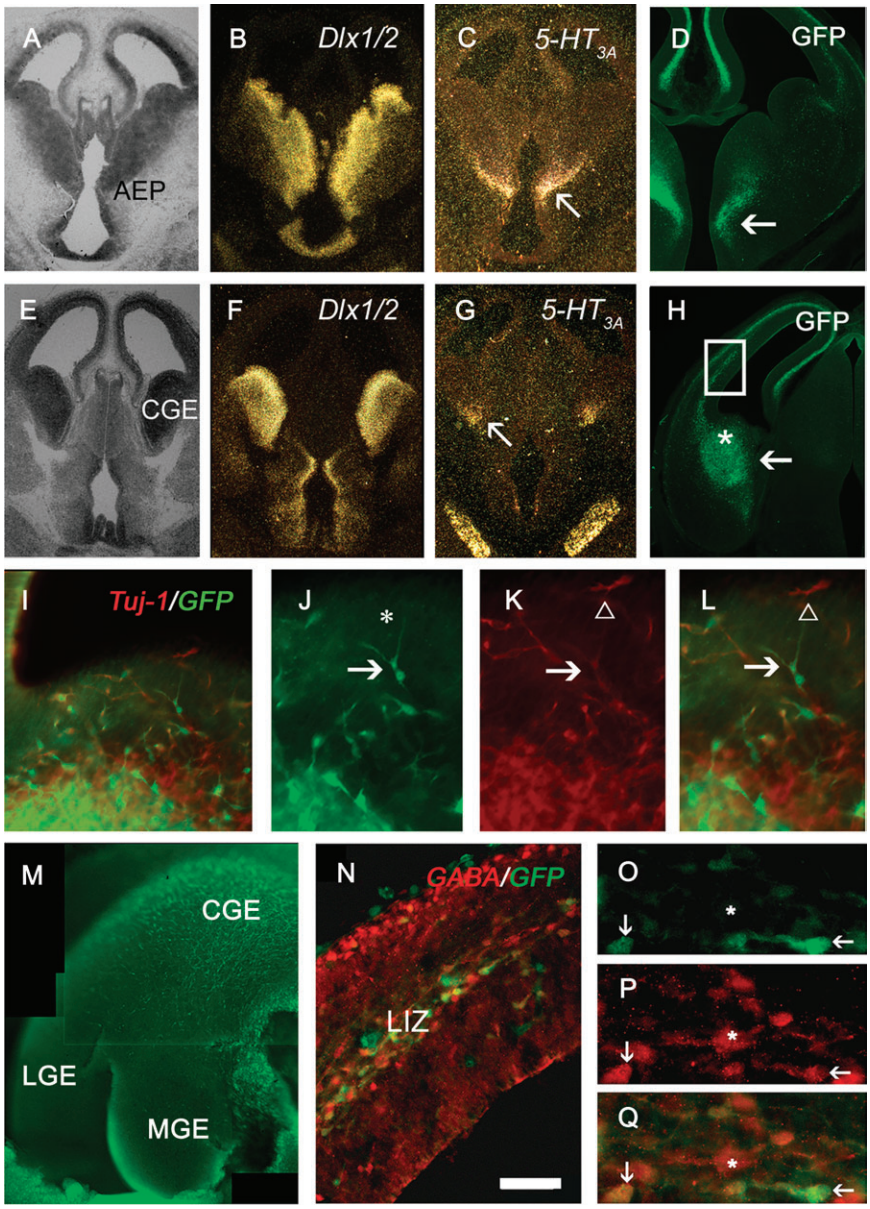

Figure 5. Expression of 5-HT_{3A} in the developing embryo at E14.5. (*A*,*E*): Brightfield coronal views of the entopeduncular area (AEP, *A*) and the caudal ganglionic eminence (CGE, *E*). (*C*,*D*,*G*,*H*): Coronal sections where arrows point to restricted expression of 5-HT_{3A} mRNA in wild-type mouse (*C*,*G*) and GFP immunostaining from a 5-HT_{3A}:GFP transgenic mouse (*D*,*H*). The main sites of 5-HT_{3A} expression where located at the telencephalic–diencephalic junction, in AEP (*A*,*B*,*D*) and in CGE (*E*,*F*,*H*). (*B*–*F*) Alternate sections of the preparations shown in (*A*,*E*) showing *Dlx1/2* expression. (*I*–*L*) Coronal section taken at the level of the CGE indicated by the asterisk in (*H*) showing cells double labeled for GFP (green) and the postmitotic marker tuj-1 (red). (*J*–*L*) Higher magnifications of the region shown in (*I*). Arrow points to a double-labeled cell and the open arrowhead points to a cell expressing only tuj-1. (*M*) Whole-mount preparation of a E14.5 5-HT_{3A}:GFP embryo showing restricted expression of GFP+ cells in the CGE. (*N*) Coronal section of the caudal cortex (boxed in *H*) of a 5-HT_{3A}:GFP embryo stained for GABA (red) showing GABA+ cells in the migratory pathway of interneurons (LIZ). (*O*–*Q*) High-power view of the section shown in (*N*). Note that only a proportion of GABA+ cells express GFP (arrows) and that all GFP+ cells in LIZ express GABA. The asterisk points to a GABA-positive cell that is not expressing GFP. LGE, lateral ganglionic eminence, LIZ, Low intermediate zone, MGE, medial ganglionic eminence. Scale bar: (*A*–*C*,*E*–*G*) 1 mm; (*D*,*H*) 800 μm; (*I*,*N*) 125 μm; (*J*–*L*) 90 μm; (*M*) 500 μm; (*O*–*Q*) 75 μm.

morphologies. Most interneurons of this second class are very similar to neurogliaform cells according to their specific electrophysiological, molecular and morphological properties.

Diversity of Neocortical 5-HT_{3A}-Expressing Interneurons

GABAergic interneurons within the neocortex are typically described and classified on the bases of their physiological, molecular, and morphological features. The large amount of data collected from the rat neocortex led to the distinction of at least 5 subclasses of interneurons according to the Petilla 2005 nomenclature (Ascoli et al. 2008; Karagiannis et al. 2009): Fast spiking (FS) cells expressing Parv, Martinotti cells expressing SOM and CB, Neurogliaform cells expressing NPY, VIP bipolar cells and large CCK basket cells.

The unsupervised clustering performed in the present study disclosed 2 main groups of 5-HT_{3A}-expressing interneurons with distinctive electrophysiological, molecular, and morphological hallmarks that were remarkably similar to those characterizing particular interneuronal subtypes previously described in the rat neocortex (Kubota and Kawaguchi 1994; Cauli et al. 1997; Cauli et al. 2000; Ascoli et al. 2008; Karagiannis et al. 2009).

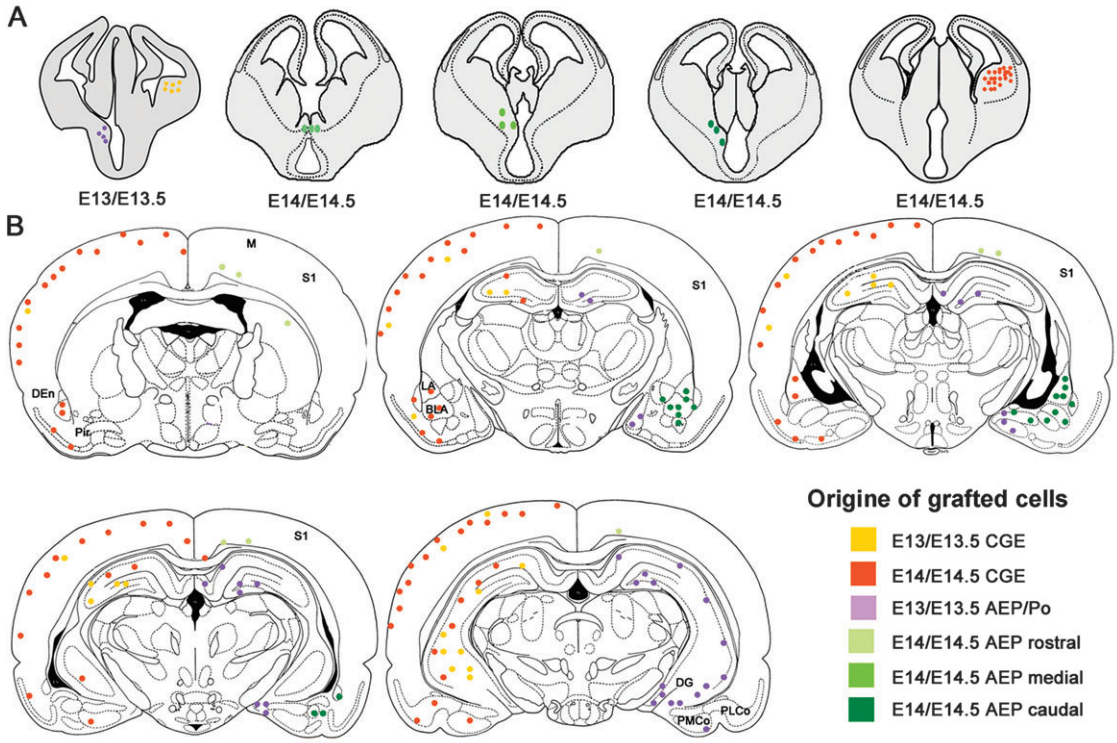

Figure 6. Distribution of 5-HT3A:GFP+ grafted cells derived from the APE/Po and CGE. (*A*) Schematic drawings indicating the regions taken for donor cells dissociation. (*B*) Schematic drawings showing the general distribution of 5-HT_{3A}:GFP+ grafted cells in the host brain (P19–P25). Amg, amygdala; BLA, basolateral amygdaloid nucleus; Cg, cingulate cortex area; DEn, dorsal endopiriform nucleus; DG, dentate gyrus; LA, lateral amygdaloid nucleus; M, motor cortex; Pir, piriform cortex; PlCo, posterolateral cortical amygdaloid nucleus; PMCo, posteromedial cortical amygdaloid nucleus; S1, somatosensory cortex.

GFP-expressing cells segregated in the VIP-cluster were never found in layer I and were characterized by the high occurrence of *VIP* and to a lower extent *CR* but the absence of *CB*, *Parv*, and *SOM*. These molecular properties match those characterizing 5-HT_{3A}-expressing interneurons in the rat neocortex (Morales and Bloom 1997; Ferezou et al. 2002). The adapting or bursting firing behavior of these cells correspond to that of VIP-expressing cells previously characterized in the rat somatosensory cortex (Bayrakter et al. 1997; Cauli et al. 1997; Porter et al. 1998). However, at high stimulation intensity, these cells did not exhibit the typical pronounced amplitude accommodation described in rat VIP-expressing neurons (Cauli et al. 2000). This divergence could be ascribable to species differences between mice and rats. On the other hand, the large majority of cells belonging to the VIP-cluster exhibited bipolar somatodendritic morphology with descending axonal arborization, morphological traits that typically correspond to the descriptions of rat VIP-expressing interneurons (Kawaguchi and Kubota 1996; Bayraktar et al. 1997).

The main characteristic of the second group of cells identified by Ward's clustering was the high expression of *NPY* (87%). Our results revealed that the electrophysiological, morphological, and molecular properties of 5-HT_{3A}-expressing neurons of the NPY-cluster were very similar to those of previously characterized neurogliaform cells (Kawaguchi 1995; Hestrin and Armstrong 1996; Zhou and Hablitz 1996; Cauli et al. 2004). Indeed, the typical physiological features of the neurogliaform interneurons are found in this group such as high rheobase, delayed firing, marked frequency adaptation at high firing rates, and pronounced amplitude accommodation during the action potentials discharge (Kawaguchi 1995; Chu et al. 2003; Simon et al. 2005; Ascoli et al. 2008; Karagiannis et al. 2009). Interestingly, *Reelin* was expressed in 52% of cells in the NPY-cluster, whereas only 23% of cells of the VIP-cluster contained this marker. These results are in agreement with immunohistochemical studies indicating that reelin is preferentially coexpressed with NPY and/or SOM (Alcántara et al. 1998; Pesold et al. 1999). Although our immunohistochemical experiments did not disclose any coexpression of GFP and SOM, the scRT-PCR results revealed the presence of *SOM* mRNA in 29% ($n = 9$ of 31) of cells within the NPY-cluster. This discrepancy could be explained by the different sensitivities of both techniques (Gallopin et al. 2006, Burkhalter 2008). Indeed, it is unlikely that neurons of the NPY-cluster that present *SOM* mRNA detection could belong to the Martinotti subtype because it has been demonstrated that Martinotti cells derive from the MGE (Butt et al. 2005; Miyoshi et al. 2007). Furthermore, this is in agreement with the absence of expression of *Lhx6* mRNAs in the GFP cells recorded and harvested. Indeed, *Lhx6* has been reported to be expressed in Parv-expressing FS interneurons and SOM Martinotti cells at mature stages (Liodis et al. 2007).

Genesis and Specification of Neocortical 5-HT_{3A}+ Interneurons

Our birth-dating experiments show that neocortical 5-HT_{3A} interneurons display a peak of genesis at E14.5 that largely precedes those observed for glutamatergic neurons in the same areas. In particular, in the superficial neocortical layers, 5-HT_{3A} interneurons are generated between E13.5 and E14.5, whereas

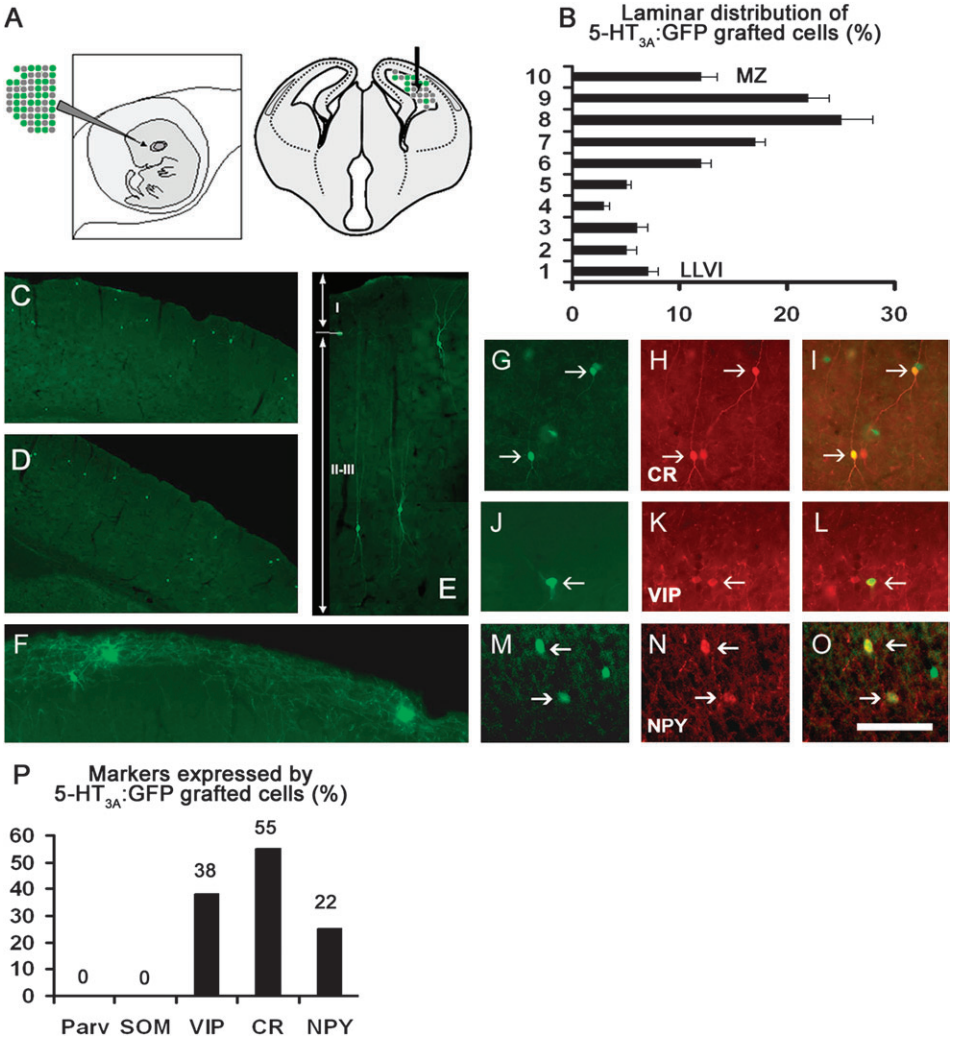

Figure 7. Fate of In utero grafted 5-HT_{3A}:GFP+ cells from the CGE at E14.5. (*A*) Schematic drawing illustrating the in utero grafting technique. (*B*) Histogram (percentage ± SEM) indicating the laminar distribution of 5-HT_{3A}:GFP+ grafted cells ($n = 235$ cells obtained from 7 grafted animals) in the somatosensory cortex. Cortical strips (500 μm width) were longitudinally subdivided into 10 equal bins from the marginal zone (MZ) to the lower part of the layer VI (LLVI). (*C*,*D*) E14 5-HT_{3A}:GFP+ CGE-derived cells give rise to numerous interneurons located in the supragranular layers of the cerebral cortex. Note that the section shown in panel (*C*) was taken from an animal that received 5-HT_{3A}:GFP+ cells that were sorted by flow cytometry. (*E*) Section showing 5-HT_{3A}:GFP+ cells located in the supragranular layers of the cortex and displaying bipolar or double bouquet morphologies. Cortical layers are indicated. (*F*) Section showing multipolar 5-HT_{3A}:GFP+ grafted cells located in cortical layer I displaying complex morphologies. (*G–O*) Neocortical grafted cells labeled for CR (*G–I*; red), VIP (*J–L*; red) or NPY (*M–O*; red) in the supragranular layers II–III. (*P*) Histogram showing the percentage of grafted cells that express different interneuronal markers in the somatosensory cortex. Throughout the cortex, the most commonly expressed markers were CR, VIP and NPY. Scale bar: (*C–D*): 700 μm; (*E*): 80 μm; (*F–O*) 100 μm.

glutamatergic neurons are generated between E15.5 and E17.5 (Bayer and Altman 1991). This is in contrast with the general view that GABAergic neurons tend to integrate the same cortical layer as projection neurons born at the same time (Miller 1986), following their typical inside-out neurogenesis gradient with early generated neurons constituting the deeper cortical layers and subsequently born neurons populating progressively more superficial layers (Angevine and Sidman 1961; Rakic 1971). Such an inside-out neurogenesis gradient has been demonstrated for Parv+ and SOM+ interneurons that account for a large majority of cortical GABAergic interneurons (Cavanagh and Parnavelas 1988; Ang et al. 2003; Rymar and Sadikot 2007), and this has masked for a long time the behavior of specific subpopulation of interneurons. Indeed, exceptions have been noticed such as VIP+ interneurons that do not show a distinct inside-out neurogenesis gradient (Cavanagh and Parnavelas 1989) and NPY+ interneurons that display a scattered neurogenesis pattern (Cavanagh and Parnavelas 1990). Moreover, CR+ interneurons have recently revealed an outside-in neurogenetic gradient (Rymar and Sadikot 2007). Together, these reports suggest that different subpopulations of cortical GABAergic neurons may use different strategies and cues for their layer targeting. Our study confirms and extends this atypical behavior to neocortical interneurons expressing 5-HT_{3A}.

Our grafting experiments demonstrate that neocortical 5-HT_{3A}-expressing interneurons are originating from the CGE. Following their ventricular transplantation into wild-type animals, the E14/E14.5 CGE-derived 5-HT3A:GFP cells adopt neurochemical phenotype, distribution, and functional properties similar to those found in intact 5-HT_{3A}:GFP mice. The fate of these interneurons is therefore determined at early developmental stages, similarly to what have been observed for other subpopulation of interneurons (Nery et al. 2002; Butt et al. 2005).

It is unclear how progenitor cells from the CGE are specified and how their pattern of migration and maturation behavior are regulated. Two nonexcluding mechanisms may account for the areal and laminar specificity of 5-HT_{3A}+ grafted interneurons. One hypothesis would be that interneurons that were not correctly positioned (i.e., inappropriate cortical lamina) would either have failed to fully differentiate or would have undergone apoptosis. In favor of this assumption, it has been shown that, in vitro, the survival of small interneurons expressing VIP/CR critically depends on glutamatergic activity during a restricted time window corresponding to the early postnatal period (de Lima et al. 2004; Vitalis et al. 2007). On the other hand, our favored hypothesis would be that a specific combination of transcription factors and guidance molecules in young postmitotic neurons would be sufficient to target one interneuron to a specific prosencephalic area and more precisely in a specific cortical lamina. Indeed, recent studies suggest that motility (Powell et al. 2001; Polleux et al. 2002; Tripodi et al. 2004) and guidance (Tripodi et al. 2004; Pozas and Ibanez 2005) of interneurons depend on several molecular cues that are at least in part differentially expressed in ganglionic eminences and cortical compartments.

The transcription factor Nr2F2 is preferentially expressed in the CGE (Tripodi et al. 2004; Kanatani et al. 2008) and plays a crucial role in specifying the typical caudal migration of CGE cells (Yozu et al. 2005). In the present study, immunocytochemistry data indicate that Nr2F2 is selectively expressed by a large proportion of migrating 5-HT_{3A}+ interneurons at E16 (Fig. S5). In addition, both our immunocytochemical and scRT-PCR results reveal that Nr2F2 expression persists in these cells at later stages (P21 and P14–18, respectively), when the 5-HT_{3A}+ interneurons have integrated the superficial cortical layers. These observations suggest that Nr2F2 is likely to play a role in the maintenance of this cell population. Hence, although the involvement of Nr2F2 in the migration of GABAergic neurons has been well described (Tripodi et al. 2004; Kanatani et al. 2008), its functional role within the mature neocortex remains to be further studied.

Our work highlights the protracted expression of the 5-HT_{3A} subunit, which is specifically expressed by 2 subtypes of neocortical GABAergic interneurons. Although various studies tend to explore the involvement of 5-HT_3 receptors on the mature neocortical network activity (Ferezou et al. 2002; Puig et al. 2004; Moreau et al. 2009), further investigations would be essential to elucidate the developmental role of these receptors in the migration and maturation behavior of CGE cells specified to give rise to VIP- and NPY-expressing neocortical interneurons. This last point would be of great interest because endogenous serotonin or maternal serotonin is known to be implicated in various aspects of brain development (Gaspar et al. 2003; Vitalis and Parnavelas 2003; Côté et al. 2007; see also Riccio et al. 2008).

Supplementary Material

Supplementary material can be found at: http://www.cercor.oxfordjournals.org/.

Funding

CNRS, INSERM, FRM, ESPCI ParisTech, and the French National Research Agency (ANR-06-NEURO-033-01 grant).

Notes

We warmly thank Dr Marie-Claude Potier for advice and support. We thank Dr Luc Maroteaux, Dr Patricia Gaspar, Dr Bruno Cauli, and Dr Olivier Cases for comments and advice. We thank Chantal Alvarez and Dragos Inta for precious technical help. We thank Dr Epelbaum for providing antisomatostatin antibodies and Dr Emerit for providing specific 5-HT_{3A} plasmid. We thank Dr Philippe Vielh for allowing us to carry out the flow cytometry purification in his laboratory and Dr Zofia Maciorowski for advice on cytometry. We thank Marie Fan and Christophe Varin, students at ESPCI, for their precious help in the project. The Tg(Htr3a-GFP)1Gsat was provided by the GENSAT Consortium (Rockeffeler University-GENSAT Consortium). *Conflict of Interest*: None declared.

References

Alcántara S, Ruiz M, D'Arcangelo G, Ezan F, de Lecea L, Curran T, Sotelo C, Soriano E. 1998. Regional and cellular patterns of reelin mRNA expression in the forebrain of the developing and adult mouse. J Neurosci. 18:7779–7799.

Anderson S, Mione M, Yun K, Rubenstein JL. 1999. Differential origins of neocortical projection and local circuit neurons: roles of Dlx genes in neocortical interneurogenesis. Cereb Cortex. 9:646–654.

Anderson SA, Marín O, Horn C, Jennings K, Rubenstein JL. 2001. Distinct cortical migrations from the medial and lateral ganglionic eminences. Development. 128:353–363.

Andjelic S, Gallopin T, Cauli B, Hill EL, Roux L, Badr S, Hu E, Tamas G, Lambolez B. 2008. Glutamatergic non-pyramidal neurons from neocortical layer VI and their comparison with pyramidal and spiny stellate neurons. J Neurophysiol. 101:641–654.

Ang ES, Jr., Haydar TF, Glucnic V, Rakic P. 2003. Four-dimensional migratory coordinates of GABAergic interneurons in the developing mouse cortex. J Neurosci. 23:5805–5815.

Angevine JB, Jr., Sidman RL. 1961. Autoradiographic study of cell migration during histogenesis of cerebral cortex in the mouse. Nature. 192:766–768.

Ascoli GA, Alonso-Nanclares L, Anderson SA, Barrionuevo G, Benavides-Piccione R, Burkhalter A, Buzsáki G, Cauli B, Defelipe J, Fairén A, et al. 2008. Petilla terminology: nomenclature of features of GABAergic interneurons of the cerebral cortex. Nat Rev Neurosci. 9:557–568.

Baraban SC, Tallent MK. 2004. Interneuron diversity series: interneuronal neuropeptides–endogenous regulators of neuronal excitability. Trends Neurosci. 27:135–142.

Bayer S, Altman J. 1991. Neocortical development. New York: Raven Press.

Bayraktar T, Staiger JF, Acsady L, Cozzari C, Freund TF, Zilles K. 1997. Co-localization of vasoactive intestinal polypeptide, gamma- aminobutyric acid and choline acetyltransferase in neocortical interneurons of the adult rat. Brain Res. 757:209–217.

Burkhalter A. 2008. Many specialists for suppressing cortical excitation. Front Neurosci. 2:155–167.

Butt SJ, Fucillo M, Nery S, Noctor S, Kriegstein A, Corbin JG, Fishell G. 2005. The temporal and spatial origins of cortical interneurons predict their physiological subtype. Neuron. 48:591–604.

Cauli B, Audinat E, Lambolez B, Angulo MC, Ropert N, Tsuzuki K, Hestrin S, Rossier J. 1997. Molecular and physiological diversity of cortical nonpyramidal cells. J Neurosci. 17:3894–3906.

Cauli B, Porter JT, Tsuzuki K, Lambolez B, Rossier J, Quenet B, Audinat E. 2000. Classification of fusiform neocortical interneurons based on unsupervised clustering. Proc Natl Acad Sci U S A. 97:6144–6149.

Cauli B, Tong XK, Rancillac A, Serluca N, Lambolez B, Rossier J, Hamel E. 2004. Cortical GABA interneurons in neurovascular coupling: relays for subcortical vasoactive pathways. J Neurosci. 24:8940–8949.

Cavanagh ME, Parnavelas JG. 1988. Development of somatostatine immunoreactive neurons in the rat occipital cortex: a combined immunocytochemical-autoradiographic study. J Comp Neurol. 268:1–12.

Cavanagh ME, Parnavelas JG. 1989. Development of vasoactive-intestinal-polypeptide-immunoreactive neurons in the rat occipital cortex: a combined immunocytochemical-autoradiographic study. J Comp Neurol. 284:637–645.
Cavanagh ME, Parnavelas JG. 1990. Development of neuropeptide Y (NPY) immunoreactive neurons in the rat occipital cortex: a combined immunocytochemical-autoradiographic study. J Comp Neurol. 297:553–563.
Chameau P, Inta D, Vitalis T, Monyer H, Wadman WJ, van Hooft JA. 2009. The N-terminal region of reelin regulates postnatal dendritic maturation of cortical pyramidal neurons. Proc Natl Acad Sci U S A. 106:7227–7232.
Chu Z, Galarreta M, Hestrin S. 2003. Synaptic interactions of late-spiking neocortical neurons in layer 1. J Neurosci. 23:96–102.
Cobos I, Long JE, Thwin MT, Rubenstein JL. 2006. Cellular patterns of transcription factor expression in developing cortical interneurons. Cereb cortex. 16(Suppl. 1):82–88.
Corbin JG, Nery S, Fishell G. 2001. Telencephalic cells take a tangent: non-radial migration in the mammalian forebrain. Nat Neurosci Rev. 4(Suppl.):1177–1182.
Côté F, Fligny C, Bayard E, Launay JM, Gershon MD, Mallet J, Vodjdani G. 2007. Maternal serotonin is crucial for murine embryonic development. Proc Natl Acad Sci U S A. 104:329–334.
Dávid C, Schleicher A, Zuschratter W, Staiger JF. 2007. The innervation of parvalbumin-containing interneurons by VIP-immunopositive interneurons in the primary somatosensory cortex of the adult rat. Eur J Neurosci. 25:2329–2340.
DeFelipe J. 1993. Neocortical neuronal diversity: chemical heterogeneity revealed by colocalization studies of classic neurotransmitters, neuropeptides, calcium-binding proteins, and cell surface molecules. Cereb Cortex. 3:273–289.
de Lima AD, Opitz T, Voigt T. 2004. Irreversible loss of a subpopulation of cortical interneurons in the absence of glutamatergic network activity. Eur J Neurosci. 19:2931–2943.
Dumitriu D, Cossart R, Huang J, Yuste R. 2006. Correlation between axonal morphologies and synaptic input kinetics of interneurons from mouse visual cortex. Cereb Cortex. 17:81–91.
Ferezou I, Cauli B, Hill EL, Rossier J, Hamel E, Lambolez B. 2002. 5-HT3 receptors mediate serotonergic fast synaptic excitation of neocortical vasoactive intestinal peptide/cholecystokinin interneurons. J Neurosci. 22:7389–7397.
Fontaine P, Changeux JP. 1989. Localization of nicotinic acetylcholine receptor alpha-subunit transcripts during myogenesis and motor endplate development in the chick. J Cell Biol. 103:1025–1037.
Gallopin T, Geoffroy H, Rossier J, Lambolez B. 2006. Cortical sources of CRF, NKB, and CCK and their effects on pyramidal cells in the neocortex. Cereb Cortex. 16:1440–1452.
Gaspar P, Cases O, Maroteaux L. 2003. The developmental role of serotonin: news from mouse molecular genetics. Nat Rev Neurosci. 4:1002–1012.
Gelman DM, Martini FJ, Pereira SN, Pierani A, Kessaris N, Marín O. 2009. The Embryonic preoptic area is a novel source of cortical GABAergic interneurons. J Neurosci. 29:9380–9389.
Gillies K, Price DJ. 1993. The fates of cells in the developing cerebral cortex of normal and methylazoxymethanol acetate-lesioned mice. Eur J Neurosci. 5:73–84.
Gupta A, Wang Y, Markram H. 2000. Organizing principles for a diversity of GABAergic interneurons and synapses in the neocortex. Science. 287:273–278.
Halabisky BE, Shen F, Huguenard JR, Prince DA. 2006. Electrophysiological classification of somatostatin-positive interneurons in mouse sensorimotor cortex. J Neurophysiol. 96:834–845.
Heintz N. 2001. BAC to the future: the use of bac transgenic mice for neuroscience research. Nat Rev Neurosci. 2:861–870.
Heintz N. 2004. Gene expression nervous system atlas (GENSAT). Nat Neurosci. 7:483.
Helmstaedter M, Sakmann B, Feldmeyer D. 2009. The relation between dendritic geometry, electrical excitability, and axonal projections of L2/3 interneurons in rat. Barrel Cortex. 19:938–50.
Hestrin S, Armstrong WE. 1996. Morphology and physiology of cortical neurons in layer I. J Neurosci. 16:5290–5300.
Inta D, Alfonso J, von Engelhardt J, Kreuzberg MM, Meyer AH, van Hooft JA, Monyer H. 2008. Neurogenesis and widespread forebrain migration of distinct GABAergic neurons from the postnatal subventricular zone. Proc Natl Acad Sci U S A. 105:20994–20999.
Jakab RL, Goldman-Rakic PS. 2000. Segregation of serotonin 5-HT2A and 5-HT3 receptors in inhibitory circuits of the primate cerebral cortex. J Comp Neurol. 417:337–348.
Jessell TM. 2000. Neuronal specification in the spinal cord: inductive signals and transcriptional codes. Nat Rev Genet. 1:20–29.
Johnson DS, Heinemann S. 1995. Embryonic expression of the 5-HT_{3A} receptor subunit, 5-HT_{3A}R-A, in the rat: an in situ hybridization study. Mol Cell Neurosci. 6:122–138.
Kanatani S, Yozu M, Tabata H, Nakajima K. 2008. COUP-TFII is preferentially expressed in the caudal ganglionic eminence and is involved in the caudal migratory stream. J Neurosci. 28: 13582–13591.
Karagiannis A, Gallopin T, Dávid C, Battaglia D, Geoffroy H, Rossier J, Hillman E, Staiger J, Cauli B. 2009. Classification of NPY-expressing neocortical interneurons. J Neurosci. 29:3642–3659.
Karube F, Kubota Y, Kawaguchi Y. 2004. Axon branching and synaptic bouton phenotypes in GABAergic nonpyramidal cell subtypes. J Neurosci. 24:2853–2865.
Kawaguchi Y. 1995. Physiological subgroups of nonpyramidal cells with specific morphological characteristics in layer II/III of rat frontal cortex. J Neurosci. 15:2638–2655.
Kawaguchi Y, Kondo Y. 2002. Parvalbumin, somatostatin and cholecystokinin as chemical markers for specific GABAergic interneuron types in the rat frontal cortex. J Neurocytol. 31:277–287.
Kawaguchi Y, Kubota Y. 1996. Physiological and morphological identification of somatostatin- or vasoactive intestinal polypeptide-containing cells among GABAergic cell subtypes in rat frontal cortex. J Neurosci. 16:2701–2715.
Kubota Y, Kawaguchi Y. 1994. Three classes of GABAergic interneurons in neocortex and neostriatum. Jpn J Physiol. 44(Suppl. 2): S145–S148.
Lambolez B, Audinat E, Bochet P, Crepel F, Rossier J. 1992. AMPA receptor subunits expressed by single Purkinje cells. Neuron. 9:247–258.
Lavdas AA, Grigoriou M, Pachnis V, Parnavelas JG. 1999. The medial ganglionic eminence gives rise to a population of early neurons in the developing cerebral cortex. J Neurosci. 19:7881–7888.
Letinic K, Zoncu R, Rakic P. 2002. Origin of GABAergic neurons in the human neocortex. Nature. 417:645–649.
Liodis P, Denaxa M, Grigoriou M, Akufo-Addo C, Yanagawa Y, Pachnis V. 2007. Lhx6 activity is required for the normal migration and specification of interneuron subtypes. J Neurosci. 27:3078–3089.
Marín O, Rubenstein JL. 2001. A long, remarkable journey: tangential migration in the telencephalon. Nat Rev Neurosci. 2:780–790.
Menezes JR, Luskin MB. 1994. Expression of neuron-specific tubulin defines a novel population in the proliferative layers of the developing telencephalon. J Neurosci. 14:5399–5416.
Miller MW. 1986. The migration and neurochemical differentiation of gamma-aminobutyric acid (GABA)-immunoreactive neurons in rat visual cortex as demonstrated by a combined immunocytochemical-autoradiographic technique. Brain Res. 393:41–46.
Miyoshi G, Butt SJ, Takebayashi H, Fishell G. 2007. Physiologically distinct temporal cohorts of cortical interneurons arise from telencephalic Olig2-expressing precursors. J Neurosci. 27: 7786–7798.
Morales M, Bloom E. 1997. The 5-HT_{3A} receptor is present in different subpopulations of GABAergic neurons in the rat telencephalon. J Neurosci. 17:3157–3167.
Moreau AW, Amar M, Le Roux N, Morel N, Fossier P. 2009. Serotoninergic fine-tuning of the excitation-inhibition balance in rat visual cortical networks. Cereb Cortex. Jul 8. [Epub ahead of print].
Nery S, Fishell G, Corbin JG. 2002. The caudal ganglionic eminence is a source of distinct cortical and subcortical cell populations. Nat Neurosci. 5:1279–1287.
Pesold C, Liu WS, Guidotti A, Costa E, Caruncho HJ. 1999. Cortical bitufted, horizontal, and Martinotti cells preferentially express and

secrete reelin into perineuronal nets, nonsynaptically modulating gene expression. Proc Natl Acad Sci U S A. 96:3217–3222.
Polleux F, Whitford KL, Dijkhuizen PA, Vitalis T, Ghosh A. 2002. Control of cortical interneuron migration by neurotrophins and PI3-kinase signaling. Development. 129:3147–3160.
Porter JT, Cauli B, Staiger JF, Lambolez B, Rossier J, Audinat E. 1998. Properties of bipolar VIPergic interneurons and their excitation by pyramidal neurons in the rat neocortex. Eur J Neurosci. 10: 3617–3628.
Powell EM, Mars WM, Levitt P. 2001. Hepatocyte growth factor/scatter factor is a motogen for interneurons migrating from the ventral to dorsal telencephalon. Neuron. 30:79–89.
Pozas E, Ibanez CF. 2005. GDNF and GFRalpha1 promote differentiation and tangential migration of cortical GABAergic neurons. Neuron. 45:701–713.
Puig MV, Santana N, Celada P, Mengod G, Artigas F. 2004. In vivo excitation of GABA interneurons in the medial prefrontal cortex through 5-HT3 receptors. Cereb Cortex. 14:1365–1375.
Rakic P. 1971. Guidance of neurons migrating to the fetal monkey neocortex. Brain Res. 33:471–476.
Riccio O, Potter G, Walzer C, Vallet P, Szabo G, Vutskits L, Kiss JZ, Dayer AG. 2008. Excess of serotonin affects embryonic interneuron migration through activation of the serotonin receptor 6. Mol. Psychiatry. 14:280–290.
Ruano D, Lambolez B, Rossier J, Paternain AV, Lerma J. 1995. Kainate receptor subunits expressed in single cultured hippocampal neurons: molecular and functional variants by RNA editing. Neuron. 14:1009–1017.
Rymar VV, Sadikot AF. 2007. Laminar fate of cortical GABAergic interneurons is dependent on both birthdate and phenotype. J Comp Neurol. 501:369–380.
Schaeren-Wiemers N, Gerfin-Moser A. 1993. A single protocol to detect transcripts of various types and expression levels in neural tissue and cultured cells: in situ hybridization using digoxigenin-labelled cRNA probes. Histochemistry. 100:431–440.
Schuurmans C, Guillemot F. 2002. Molecular mechanisms underlying cell fate specification in the developing telencephalon. Curr Opin Neurobiol. 12:26–34.
Simon A, Olah S, Molnar G, Szabadics J, Tamas G. 2005. Gap-junctional coupling between neurogliaform cells and various interneuron types in the neocortex. J Neurosci. 25:6278–6285.
Soriano E, Cobos A, Fairen A. 1989. Neurogenesis of glutamic acid decarboxylase immunoreactive cells in the hippocampus of the mouse. I: region superior and region inferior. J Comp Neurol. 281: 586–602.
Tamas G, Buhl EH, Somogyi P. 1997. Fast IPSPs elicited via multiple synaptic release sites by different types of GABAergic neurone in the cat visual cortex. J Physiol. 500(Pt 3):715–738.
Tecott LH, Maricq AV, Julius D. 1993. Nervous system distribution of the serotonin 5-HT3 receptor mRNA. Proc Natl Acad Sci U S A. 90:1430–1434.
Thorndike RL. 1953. Who belongs in the family? Psychometrika. 18:267–276.
Tripodi M, Filosa A, Armentano M, Studer M. 2004. The COUP-TF nuclear receptors regulate cell migration in the mammalian basal forebrain. Development. 131:6119–6129.
Vitalis T, Cases O, Passemard S, Callebert J, Parnavelas JG. 2007. Embryonic depletion of serotonin affects cortical development. Eur J Neurosci. 26:331–344.
Vitalis T, Parnavelas JG. 2003. The role of serotonin in early cortical development. Dev Neurosci. 25:245–256. Review.
Ward JH. 1963. Hierarchical grouping to optimize an objective function. J Am Stat Assoc. 58:236–244.
Wichterle H, Garcia-Verdugo JM, Herrera DG, Alvarez-Buylla A. 1999. Young neurons from medial ganglionic eminence disperse in adult and embryonic brain. Nat Neurosci. 2:461–466.
Xu Q, de la Cruz E, Anderson SA. 2003. Cortical interneuron fate determination: diverse sources for distinct subtypes? Cereb Cortex. 13:670–676.
Yozu M, Tabata H, Nakajima K. 2005. The caudal migratory stream: a novel migratory stream of interneurons derived from the caudal ganglionic eminence in the developing mouse forebrain. J Neurosci. 25:7268–7277.
Zhou FM, Hablitz JJ. 1996. Morphological properties of intracellularly labeled layer I neurons in rat neocortex. J Comp Neurol. 376: 198–213.